Fall 2024

Rhizaria marine protists are unexpectedly abundant and exhibit taxonomic and trophic diversity in the northern Gulf of Alaska

Jaime Blais
Western Washington University, jrblais3@gmail.com

Rhizaria marine protists are unexpectedly abundant and exhibit taxonomic and trophic diversity in the northern Gulf of Alaska

By

Jaime Blais

Accepted in Partial Completion

of the Requirements for the Degree

Master of Science

ADVISORY COMMITTEE

Dr. Suzanne Strom, Chair

Dr. Shawn Arellano

Dr. Brady Olson

GRADUATE SCHOOL

Dr. David L. Patrick, Dean

Master's Thesis

In presenting this thesis in partial fulfillment of the requirements for a master's degree at Western Washington University, I grant to Western Washington University the non-exclusive royalty-free right to archive, reproduce, distribute, and display the thesis in any and all forms, including electronic format, via any digital library mechanisms maintained by WWU.

I represent and warrant this is my original work and does not infringe or violate any rights of others. I warrant that I have obtained written permission from the owner of any third party copyrighted material included in these files.

I acknowledge that I retain ownership rights to the copyright of this work, including but not limited to the right to use all or part of this work in future works, such as articles or books.

Library users are granted permission for individual, research and non-commercial reproduction of this work for educational purposes only. Any further digital posting of this document requires specific permission from the author.

Any copying or publication of this thesis for commercial purposes, or for financial gain, is not allowed without my written permission.

Jaime Blais

October 2024

Rhizaria marine protists are unexpectedly abundant and exhibit taxonomic and trophic diversity in the northern Gulf of Alaska

A Thesis

Presented to

The Faculty of

Western Washington University

In Partial Fulfillment

Of the Requirements for the Degree

Master of Science

by

Jaime Blais

October 2024

Abstract

Rhizaria are a diverse group of large (~50 µm to 5 mm) hetero- and mixotrophic amoeboid marine protists that are often overlooked due to their lower abundances and wide size range relative to other plankton, and fragility. Despite the global distribution of these unique protists, the fundamentals of their biology and ecology are poorly understood due to an insufficient number of datasets and differing methodologies. Rhizaria have been a missing puzzle piece of the protist community in the northern Gulf of Alaska (NGA). Understanding their ecology will provide a more complete picture of trophodynamics in this subarctic marine ecosystem. The NGA is a variable yet productive region that is experiencing a long-term warming trend. Therefore, it is important to monitor protist assemblages because a shift in community composition could reverberate up to higher trophic levels and impact food web resiliency. Changes in food web dynamics could also affect the viability of Alaskan fisheries, an industry of high importance to the economy and food security of the US. The Rhizaria infrakingdom encompasses organisms that biomineralize silica, calcium carbonate, or strontium sulfate skeletons or tests. The skeletal features, large sizes, and substantial biomass of these amoeboid protists, which use sticky pseudopodal networks to capture prey, allow Rhizaria to facilitate carbon export and influence biogeochemical cycling. In addition to feeding on fellow plankton like diatoms, tintinnids, and copepods, some Rhizaria have symbiotic relationships with algal cells which may aid survival in offshore regions of the NGA that are iron-limited. Since they simultaneously act as predator, prey, and algal host, Rhizaria are food web scaffolders connecting microbial and protist networks to higher trophic levels. Here we present the first characterization of Rhizaria ecology in the NGA. Seawater samples were collected from CTD-secured Niskin bottles at stations within the NGA Long-Term Ecological Research (LTER) study area during summer 2023, concentrated by reverse filtration with 50 µm mesh, and analyzed with inverted epi-fluorescence microscopy. It was discovered that different taxonomic groups inhabited distinct depth niches. Foraminifera dominated surface waters, Radiolaria exhibited a more cosmopolitan vertical distribution, and Cercozoa were the deepest living. We report some of the highest Rhizaria abundances from any ocean environment to date; peak abundance in the NGA was 25 cells L^{-1}. Acantharia dominated

the Rhizaria community and were widespread throughout the water column and across the gulf. Phytoplankton and microzooplankton were common prey types of Rhizarians. Incidences of prey capture and algal association were more likely to occur near the surface and in offshore waters. With the addition of this northeastern North Pacific dataset to the growing body of work globally, we suggest a restructuring of the current understanding of Rhizaria biogeographical distributions to one where abundances near the poles are similar to the equatorial region. This study contributed to a broader understanding of trophodynamics and protist diversity in the NGA with the incorporation of Rhizaria into the food web for the first time. We highlight Rhizaria as key players in NGA food web dynamics as evidenced by their wide distributions, diversity, and unique nutrition strategies.

Acknowledgements

First and foremost, I thank my New England family and friends for their unwavering support in my pursuit of a career in marine science over the past decade, particularly this portion of my journey. Thank you to my newfound Bellingham community of friends, who were incredibly supportive and made my time in Washington unforgettable; you are immensely difficult to leave behind (for now). To my Biology cohort, thank you for being an unexpected, amazing group of friends and a critical support system; I will treasure our bond forever.

Thank you to my advisor Dr. Suzanne Strom for fostering my growth as a marine scientist and for giving me an incredible opportunity to work with an interdisciplinary oceanographic research group; one that came with once-in-a-lifetime experiences that I will never forget. Her guidance and expertise were critical to my success. Thank you to Dr. Shawn Arellano and Dr. Brady Olson for serving on my committee. I value their perspectives, which made me think more deeply about my work and what it all means. I also thank Shannon Point Marine Center staff for helping me with various research things, especially senior lab members Kerri Fredrickson and Kelley Bright for their advice and friendship; they were wonderful women scientists to learn from and look up to.

Finally, thank you to the scientists of the NGA-LTER for welcoming me into their network; they were a true source of inspiration. I thank Katey Williams, Asher Marvy, and Kaleigh Ballentine for helping me carry dozens of seawater-filled buckets up flights of stairs at-sea. Thank you to the crew of R/V *Kilo Moana* for facilitating this research and maintaining safety and wellbeing aboard the ship. This project was funded by the National Science Foundation, the North Pacific Research Board, the Alaska Ocean Observing System, Gulf Watch Alaska, and Western Washington University's Office of Research and Sponsored Programs.

Table of Contents

List of Tables

List of Figures

Introduction

Scientists have been uncovering the biology and ecology of Rhizaria for at least the last 150 years. A supergroup of large (roughly 50 µm to 5 mm), amoeboid, hetero- and mixotrophic marine protists, Rhizaria are characterized by pseudopodal cytoplasmic projections and intricate skeletal structures made of either silica, (Polycystina and Phaeodaria), calcium carbonate (Foraminifera), or strontium sulfate (Acantharia). Although Rhizaria are found globally in marine ecosystems, the fundamentals of their biology and ecology are poorly understood, especially in the northern Gulf of Alaska where formal sampling initiatives to effectively target these protists have been lacking. Only a few studies have taken place in the Gulf of Alaska at station PAPA (50°N 145°W), but these were vertical flux analyses (Takahashi 1987, 1997) which did not address the ecology of living planktic Rhizaria.

The Northern Gulf of Alaska Long-Term Ecological Research (NGA-LTER) study area extends about 200 km off the south-central coast of Alaska (Figure 1), spanning the continental shelf to the open ocean. This region is a productive subarctic marine ecosystem with a semi-predictable spring phytoplankton bloom, considerable copepod and gelatinous zooplankton biomass, and multiple critically important fish populations like walleye pollock (Dorn et al. 2017, Strom 2023). Alaskan fisheries brought home $1.48 billion worth of catch in 2020, which accounted for more than half of the total US landings (NMFS 2022). Rhizaria likely help support the NGA food web and the food sources generated from it. These large protists likely connect and transfer biomass to multiple trophic levels, act as both predator and prey, host symbiotic microalgae, facilitate ballasting and carbon export, and help sustain food webs in nutrient-limited regions through mixotrophy (Suzuki and Not 2015, Biard et al. 2016, 2018, Guidi et al. 2016, Boltovskoy et al. 2017, Stoecker et al. 2017, Monferrer et al. 2020). These ocean processes will likely be impacted by climate change. The NGA has experienced a long-term warming trend, including recent heat waves (Danielson et al. 2022, Strom 2023). Therefore, it is important to track the composition of protist assemblages because any perturbations to the community could reverberate up the food web and impact Alaskan fisheries.

Rhizaria are now being recognized as important players in the biological carbon pump, biogeochemical cycling, and trophodynamics. Due to their large sizes, inorganic skeletons, and global distribution (Suzuki and Not 2015, Biard et al. 2016, 2018, Guidi et al. 2016, Boltovskoy et al. 2017, Stoecker et al. 2017, Monferrer et al. 2020) these amoeboid protists, especially the large and/or colonial species, facilitate particle ballasting and carbon and biogenic silica export (Lampitt et al. 2009, Guidi et al. 2016, Biard et al. 2018, Stukel et al. 2018, Gutierrez-Rodriguez et al. 2019, Ikenoue et al. 2019). They also connect microbial and protist networks to higher trophic levels as predators of phytoplankton and microzooplankton, prey for macrozooplankton and fish, and host to mutualistic or commensal algal cells. Rhizaria feed opportunistically on a variety of planktonic organisms throughout the water column including diatoms, tintinnids, and nauplii (Swanberg and Caron 1991). Sticky, tendril-like pseudopodia protrude radially from the endoplasm of the cell and are used to capture prey, which are then phagocytized (Kimoto 2015, Suzuki and Not 2015, Boltovskoy et al. 2017). Regarding the reverse trophic dynamic, there have only been a handful of reports on Rhizaria as prey themselves. The gut contents of various marine plankton and nekton contained Rhizaria: crustaceans such as mysids, euphausiids, amphipods, and copepods (Hopkins 1985, 1987, Gowing and Wishner 1986), salps (Hopkins and Torres 1989, Gowing 1989), liparid fish (Takami and Fukui 2012) and deep-sea smelt (Hopkins and Torres 1989).

In addition to feeding, many surface-dwelling Radiolaria and Foraminifera host symbiotic algae such as cyanobacteria (*Synechococcus* sp. and *Prochlorococcus* sp.), haptophytes, and dinoflagellates, making them mixotrophs (Decelle et al. 2015). Mixotrophic protists help sustain food webs and may aid in resilience in resource-limited regions because they are capable of transitioning between nutrition strategies depending on environmental conditions or prey availability (Stoecker et al. 2017, Strom et al. 2024). Photosymbionts provide Rhizaria with carbon for use in maintenance metabolism or growth (Swanberg 1983, Stoecker et al. 2017). The offshore NGA waters are typically high in nitrate but are iron-limited, resulting in low phytoplankton biomass or chlorophyll. These conditions restrict primary

productivity and availability of phytoplankton prey, especially larger cells (Nishioka et al. 2021). Therefore, Rhizaria-algal relationships likely support the food web in offshore NGA waters.

Biogeographical and bathymetric faunal zones or provinces have been assigned to Radiolaria, Foraminifera, and Phaeodaria species many times in an attempt to categorize the distributions of these relatively rare protists; important influences on their biogeographical distribution appear to be latitude, temperature, and/or water mass movements (Casey 1966, 1971, Kling 1966, Renz 1976, Be 1977, Boltovskoy and Correa 2016, 2017), nutrients, and primary productivity (Boltovskoy et al. 2017). The general consensus is that Radiolaria, and to a lesser extent Phaeodaria (data are lacking), are more likely to be found in open ocean high salinities (Boltovskoy et al. 2017) and are in greatest abundance and diversity near the equator, diminishing toward the poles (Casey 1966, 1971, Petrushevskaya 1971, Renz 1976, Be 1977, Boltovskoy and Correa 2017). Foraminifera are slightly different in that abundances tend to be higher at intermediate latitudes (15-30°N) (Boltovskoy et al. 2017). Rhizaria occupy virtually all depths across the world's ocean from the surface to the depths of ocean trenches. Many Phaeodaria and select Radiolaria species have been found as deep as 8000 m at the bottom of the Kuril-Kamchatka Deep trench (Reshetnyak 1955, Nakamura and Suzuki 2015, Boltovskoy et al. 2017). The longstanding view of Polycystine Radiolaria water column distributions is that abundances are highest in the upper 100 m and decrease with depth (Boltovskoy et al. 2017). It has been said that Foraminifera follow chlorophyll distributions and stay above the thermocline (Kimoto 2015), while Phaeodaria Cercozoans are the deepest ocean dwellers out of the Rhizaria supergroup, usually residing below 300 m (Reshetnyak 1955, Nakamura and Suzuki 2015, Boltovskoy et al. 2017). This study challenges the current understanding of Rhizaria biogeographical distributions across the Pacific and Southern Oceans with the addition of our northeast North Pacific dataset.

Despite the ubiquity of Rhizaria, our understanding of their ecology and biogeographical patterns is poor for multiple reasons. Abundances are relatively low compared to more widely-studied plankton and sampling challenges exist due to the group's wide size range and biomineralized skeleton fragility (Suzuki and Not 2015, Boltovskoy et al. 2017). Since the time of the 1870s Challenger Expedition, when

the first seminal works on Rhizaria ecology and diversity were published, most sea-going scientists have utilized the plankton net-tow method or opted for sediment traps to measure distributions and flux (Haeckel 1887, Kling 1979, Takahashi and Honjo 1981, Morley and Stepien 1985, Boltovskoy and Riedel 1987, Takahashi 1987, 1997, Bernstein et al. 1990, Kling and Boltovskoy 1995, Okazaki et al. 2004, 2005, Ishitani and Takahashi 2007, Itaki et al. 2008, Ikenoue et al. 2012, 2019). More recently, *in situ* imaging instruments like the Underwater Vision Profiler 5 and 6 (Picheral et al. 2010, 2022) have been used to estimate distributions, biomass, and flux of >600 µm Rhizarians (Biard et al. 2016, 2018, Stukel et al. 2018, Biard and Ohman 2020, Llopis Monferrer et al. 2022), omitting cells in the lower half of the size range. The traditional plankton tow method has been the most common way to sample Rhizaria but can underestimate abundances and disrupt skeletons. The Acantharia subgroup produces delicate strontium sulfate skeletons that are vulnerable in net sampling and require strontium addition in samples to prevent dissolution (Beers and Stewart 1970, Michaels 1988). The under-sampling by net tows of not just Acantharians, but other Radiolarians as well as Foraminiferans, has been quantitatively demonstrated by Michaels (1988) and Stoecker et al. (1996). The goal with our sampling strategy was to capture the entire size range and not discriminate against sensitive taxa. Therefore, we employed a meticulous protocol involving Niskin bottle water collection, reverse concentration by gentle siphoning, and formalin-strontium fixation, an approach inspired by Gowing and Garrison (1992) and Stoecker et al. (1996).

This study addresses a large gap in our understanding of Rhizaria ecology in the North Pacific Ocean and, more broadly, Acantharia and Taxopodida ecology worldwide. The majority of Rhizaria plankton research to date has focused on Polycystine Radiolaria and Foraminifera. Studies conducted in the northwest and northeast North Pacific Ocean (Reshetnyak 1955, Takahashi 1987, 1997, Bernstein et al. 1990, Okazaki et al. 2003, 2004, 2005, Ishitani and Takahashi 2007, Itaki et al. 2008, Ikenoue et al. 2012, 2019), the central North Pacific gyre and equatorial region (Bradshaw 1959, Petrushevskaya 1971, Beers and Stewart 1971, Beers et al. 1975, 1977, 1982, Renz 1976, Kling 1979, Takahashi and Ling 1980, Boltovskoy and Jankilevich 1985), and the California Current Ecosystem (Casey 1966, Cleveland 1984,

Boltovskoy and Riedel 1987, Welling et al. 1992, Kling and Boltovskoy 1995), all lack data pertaining to the other major Radiolaria groups, Acantharia and Taxopodida. Taxopodida have been overlooked to an even greater extent than Acantharia; this may be because for many years their membership in the Rhizaria supergroup was contested, and they were instead classified as Heliozoans (Cachon and Cachon 1978). Therefore, Taxopodida were likely left out of sampling or unidentified by researchers, so our understanding of their distribution and abundances is primitive. More attention has been paid to this group in recent years, however, and they are now considered to be Radiolarians on the basis of phylogenetic and evolutionary analyses (Cavalier-Smith 1993, Nikolaev et al. 2004, Krabberød et al. 2011, 2017). Taxopodida are prevalent in the Southern Ocean (Gowing 1989, González 1992, Gowing and Garrison 1992), equatorial Pacific (Takahashi and Ling 1980), Eastern Indian Ocean (Munir et al. 2020, 2021), and Norwegian fjords (Ikenoue et al. 2023).

Rhizaria are important to the oceanic food web and carbon pump in other systems, so we sought to better understand their role in an unstudied subarctic region of the North Pacific, the NGA, through investigation of their ecology, biology, and diversity. We produced a comprehensive summary of Rhizaria ecology that included the first quantitative analysis of summer abundances and biomass in the context of cross-shelf and water column distributions, paired with community composition and depth-niche analyses, morphotypes, light microscope imagery, and incidences of prey capture and algal cell association. Although abundances elsewhere in the Pacific Ocean have been reported, there has not been a sufficient number of distribution studies using the same methodology to know with certainty just how prevalent Rhizaria are there. We wanted to better understand Rhizaria abundances and ocean zone distributions by generating a new subpolar dataset to incorporate into the current global biogeographical model. The current paradigm holds that abundances are greatest in the equatorial regions and decline toward the poles, so we expected low numbers of Rhizaria in the NGA. The other purpose of this study was to address the gaps in knowledge of under-sampled Rhizarians like Acantharia and Taxopodida.

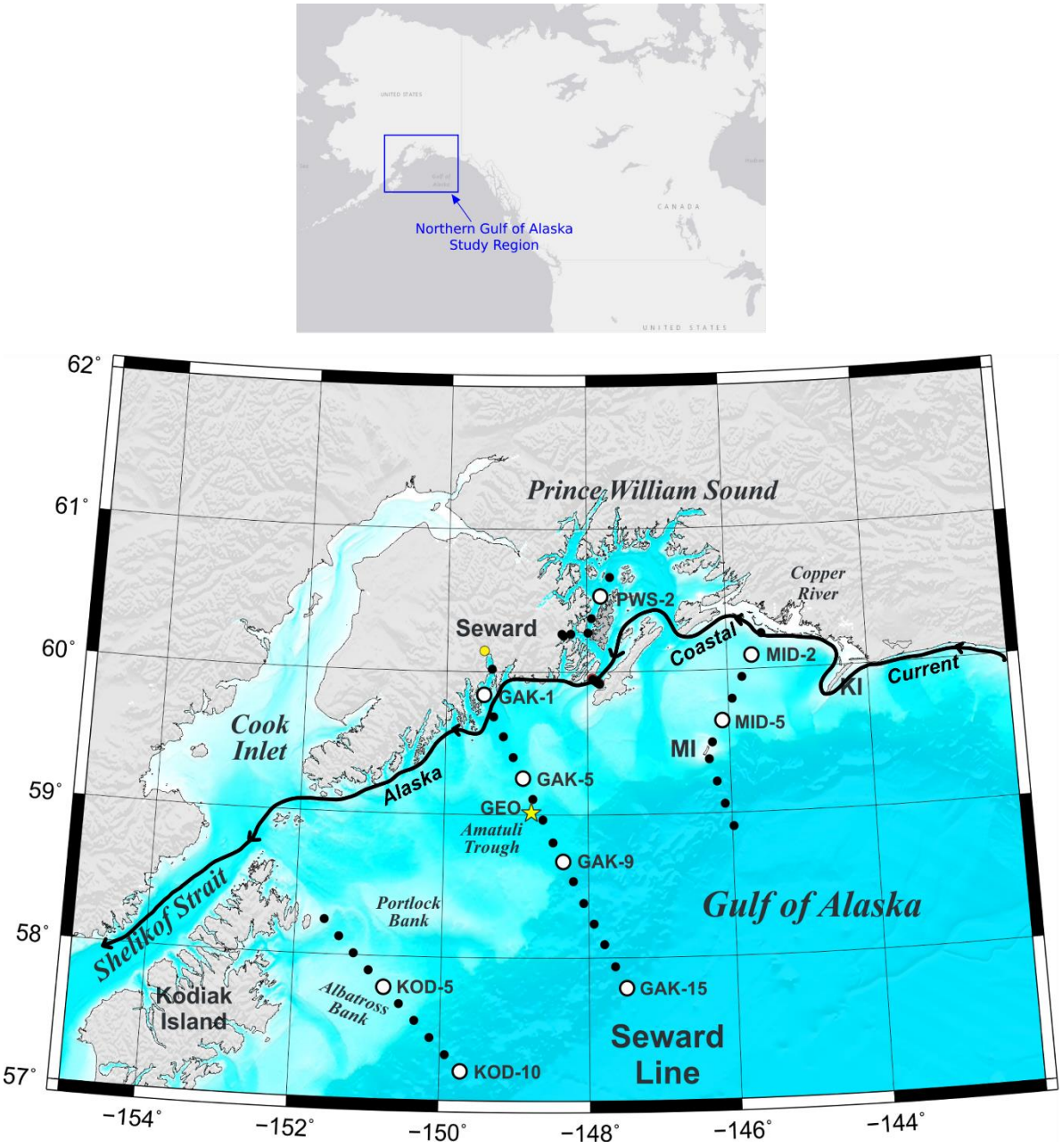

Figure 1. Northern Gulf of Alaska Long-Term Ecological Research study region. Samples were collected at four stations along the Seward Line: GAK1, GAK5, GAK9, and GAK15.

Methods

Field sampling

This research project was conducted as part of the Northern Gulf of Alaska Long-Term Ecological Research Program (NGA LTER). Seawater samples were collected between June 29 and July 6, 2023 on R/V *Kilo Moana* from CTD-secured Niskin bottles along the Seward transect line at "Gulf of Alaska" stations GAK1, GAK5, GAK9, and GAK15 (Figure 1). Four 35.25 L depth interval samples were collected at each station. Each sample held water from three combined 12 L Niskin bottles; each bottle contained water from a different depth for a total of three combined depths per depth interval sample (e.g. 0-20 m sample had water from 0, 10, and 20 m; see Table 1). Chosen depth intervals depended on bottom depth at station but together represented most of the water column. Seawater was gently transferred from Niskin bottles into buckets with lids, then reverse concentrated with siphoning through a 50 µm mesh sieve at 10°C, modeled after Gowing (1989) and Stoecker et al. (1996). Each ~35 L sample was concentrated in two stages to a final volume of 400 mL, fixed with 2% formalin (20% formaldehyde buffered with 100 g L^{-1} hexamethylenetetramine) + 0.16 mg mL^{-1} strontium chloride (Stoecker et al. 1989, 1996), and stored at 4°C. This concentration of $SrCl_2$ was used to achieve a strontium level 10x that of normal seawater to prevent dissolution of Acantharian skeletons (Beers and Stewart 1970). The Niskin bottle collection method was chosen as the best approach to quantitatively sample Rhizaria on the basis that plankton net tows can underestimate abundances and damage fragile skeletons, especially those of Acantharians (Michaels 1988, Gowing 1989, Michaels et al. 1995, Stoecker et al. 1996).

Oceanographic parameters were measured at every GAK station along the Seward Line. Salinity and temperature were measured with Sea-Bird SBE 4C conductivity and SBE 3P temperature sensors, respectively. Size-fractionated chlorophyll-a concentrations were measured at 0, 10, 20, 30, 40, 50, and 75 m. Seawater samples (280 mL) were filtered sequentially onto a 47 mm, 20 µm pore size polycarbonate membrane and a 25 mm glass fiber filter (effective pore size 0.7 µm) to separate the phytoplankton community into <20 µm and >20 µm size fractions. Chlorophyll-a was extracted with

90% acetone for 24 h at -20°C in the dark and analyzed fluorometrically (Turner Designs 10AU) using the acidification method and quantified to µg L^{-1} (Welschmeyer 1994). Beam transmission was measured with a Wetlabs C-Star 25 cm transmissometer. Nitrate concentrations were measured at the University of Alaska Fairbanks Nutrient Analytical Facility following procedures outlined in the GO-SHIP Repeat Hydrography Nutrient Manual (Becker et al. 2020). Analyses were performed on a continuous-flow QuAAtro39 AutoAnalyzer (Seal Analytical) with low detection limits (nitrate + nitrite, N+N: 0.05 µM). Finally, primary productivity was estimated from uptake of 13C-bicarbonate in 24 h deck board incubation experiments following the methods of Hama et al. (1983) and Imai et al. (2002). Experiments were duplicated to compare production of <3 µm and >3 µm phytoplankton cells. One set of samples was size-fractionated by filtering through 20 µm Nitex mesh followed by 3 µm polycarbonate membranes before collecting cells onto glass fiber filters (GFFs) (0.7 µm effective pore size). The other set of samples was collected directly onto GFFs. All GFFs were acid-fumed, dried, and analyzed for 13C/12C ratios and particulate organic carbon content at the UC Davis Stable Isotope Facility. C:chl conversion factors were determined with light microscope analysis and used to calculate phytoplankton carbon in µg C L^{-1} (Strom et al. 2016).

Rhizaria sample analysis

Samples underwent a two-stage settling process in preparation for inverted light microscope analysis. Only one-fourth of the sample volume (100 mL) was analyzed. Each sample was settled for 48 h at 4°C in a 500 mL conical tube. 90 mL was removed with a peristaltic pump and the remaining 10 mL of settled material was carefully resuspended by mixing and transferred with a Pasteur pipette into a cylindrical chamber where it settled for 48 h at 4°C. To allow for nuclei visualization, 1 mL of 10 µg mL^{-1} DAPI stain was also added to the final sample volume during the second settling stage. Rhizarians were identified, counted, and measured with an eyepiece micrometer under light microscopy (Zeiss IM 35) at 200x and 320x. Photographs were taken with a Google Pixel 6 camera (50 MP, f/1.9, 25 mm). Each individual was classified to at least infra/subphylum level (Cercozoa, Foraminifera, and Radiozoa also

known as Radiolaria) based on the phylogeny of Cavalier-Smith (2018) and (Nakamura et al. 2020) by referring to numerous visual guides (Nigrini and Moore, Jr. 1979, Kling and Boltovskoy 1999, Lee et al. 2000, Suzuki et al. 2009, Kimoto 2015, Nakamura and Suzuki 2015, Suzuki and Not 2015, Takagi et al. 2019, Munir et al. 2020, Mansour et al. 2021, Laget et al. 2023) to identify unique morphological and subcellular features of each group, which are outlined in Table 2. Subsequent lower taxonomic classifications were assigned where possible, including to class, order, family, and to species in two cases (*Sticholonche zanclea* and *Protocystis acornis*). Those individuals that could not be identified as belonging to a particular taxon but still displayed Rhizaria characteristics were classified as "Unknown Rhizaria". Additionally, morphotypes were identified within each taxonomic group based on differences in appearance, morphology, and size of the endoplasm and spines. It is likely that some morphotypes represent different life stages or morphological variants of the same species.

Epi-fluorescence illumination utilizing UV and blue excitation wavelengths (to visualize blue-fluorescing DAPI and yellow-to-red fluorescing photopigments, respectively) was used to confirm presence of protists alive at the time of fixation, including algal cells associated with Rhizaria. This method of observing DAPI-stained nuclei and autofluorescent algal cells has been effective in Radiolaria and Phaeodaria (Gowing 1989, Takahashi et al. 2003, Suzuki et al. 2009). In this study, positive incidence of algal cell association was defined as widespread, yellow-to-red fluorescence that emanated from within the endoplasm of the central capsule for Radiolaria or chambers for Foraminifera. Algal cells interacting with Rhizarians also presented as small (< ~5 µm) fluorescent puncta inside the central capsule or chambers. Hosts often exhibited both widespread fluorescence and more defined, bright puncta. In Acantharians, symbionts colonize either the extracapsulum (the cytoplasmic region outside the central capsule), or the intracapsulum (the endoplasm within the central capsule) and are contained in perialgal vacuoles (Anderson 1983, Suzuki and Not 2015, Decelle and Not 2015). Foraminifera also contain their symbionts in perialgal vacuoles, which are located in the cytoplasm-rhizopodial network and, through rhizopodial streaming by the host, can be moved inside the shell (Hemleben et al. 1989). In this study, however, we could not determine whether the widespread autofluorescence or small puncta

seen in Rhizarians represented truly symbiotic algal cells versus commensals or hitchhikers, so these incidences were defined as algal cell associations or interactions.

Rhizarians with captured prey items were also identified. For Radiolaria and Foraminifera, positive incidence of prey capture was defined as an organism of an identifiable nature (e.g., diatom, tintinnid, etc.) with a nucleus and other intracellular material (i.e. not an empty diatom frustule), or if unknown, with a nucleus and clear cell boundaries, that was visibly stuck through the Rhizarian's spines/spicules (which are attached to the sticky, cytoplasmic pseudopodal network), and/or to the central capsule/shell. Additional evidence of prey capture was the presence of large (> ~5 µm) autofluorescent puncta or regions within the central capsule of Acantharians (only three cases) or within the phaeodium vacuoles of Challengeridae that indicated ingested algal prey.

Biovolume measurements and biomass calculations

Geometric equations from Hillebrand et al. (1999) were used to calculate biovolumes of Rhizarians that had nuclei, based on an assigned shape (Table 2). Individuals without DAPI-staining nuclei were omitted from biovolume and biomass analyses because these were assumed to be empty skeletons and/or dead cells. Nuclei are located in the endoplasm of the central capsule of Radiolarians (Anderson 1983, Suzuki and Not 2015) and in the intra-shell cytoplasm of Foraminifera (Hemleben et al. 1989, Schiebel and Hemleben 2005); therefore, DAPI stain elucidated key aspects of cell structure and organization. Where applicable, ectoplasm (usually deteriorated or not visible), pseudopodia/axopodia extensions, and spicules/spines were not included in biovolume measurements; this is now common practice (Stukel et al. 2018, Ikenoue et al. 2019, Mansour et al. 2021). Supplemental Table 1 further details the geometric equations and taxon-specific cell dimensions used to calculate biovolumes. Sufficient carbon density data for Rhizarians are lacking. To our knowledge, there have been just three analyses reported to date: Michaels et al. (1995), Mansour et al. (2021), and Laget et al. (2023). These studies collected Rhizarian specimens of varying taxonomic groups from different marine systems and had at least one case of small sample size. Nonetheless, carbon density values determined by these

researchers were used to calculate the biomass of each individual in this study as outlined in Table 2. The most relevant conversion factors were chosen for each group, based either on sample collection location or morphological/taxonomic similarity. Mansour et al. (2021) compiled various Mediterranean Sea and Southern Ocean Nassellarians and obtained a carbon density value ~150x greater than that of Laget et al. (2023) (1.472 vs. 0.0089 pg C μm^{-3}, respectively). Laget et al. (2023) collected "large" *Phlebarachnium* sp. Nassellarians with gelatinous matrices (Llopis Monferrer et al. 2024). Even though we did not identify any Nassellarians that resembled this genus' morphology, 0.0089 pg C μm^{-3} was used because not only is it a small value that resulted in conservative biomass estimates for this taxon, but the samples used in that analysis were from California coastal waters in the California Current Ecosystem (CCE), a system that shares the eastern Pacific Ocean with the NGA. This Nassellaria conversion factor was also used in biomass calculations for Unknown Rhizaria because it was the lowest carbon density out of the suite used in this study, yielding conservative biomass estimates for these individuals. The carbon density of *Protocystis* sp. collected from the CCE was used to calculate biomass of Challengeridae and *Protocystis acornis*. Challengeridae and *Protocystis s*p. carbon densities determined by Mansour et al. (2021) were again not as relevant for our use because the locations of sample collection (Mediterranean Sea and Southern Ocean) were ecologically distinct, and physically distant from, the NGA. Finally, the Acantharia carbon density value was used to calculate biomass of *Sticholonche zanclea* (Taxopodida) cells because the groups share similar morphologies.

Community analysis

The relationship between Rhizaria communities at different station depths was assessed using the vegan community ecology package (v2.6.6.1; Oksanen et al. 2024) performed in R Statistical Software (v4.4.1; R Core Team 2024). Communities were compared using abundance data in a two-dimension non-metric multidimensional scaling ordination ("metaMDS" function) with the Bray-Curtis dissimilarity index (stress=0.112, non-metric fit R^2=0.987).

Table 1. Locations and depths for Rhizaria sampling (n=16).

Station	Depth interval (m)	Depths sampled
GAK1	0-20	0, 10, 20
	30-50	30, 40, 50
	60-80	60, 70, 80
	100-250	100, 150, 250
GAK5	0-20	0, 10, 20
	30-50	30, 40, 50
	60-80	60, 70, 80
	90-150	90, 100, 150
GAK9	0-20	0, 10, 20
	30-50	30, 40, 50
	60-80	60, 70, 80
	100-250	100, 150, 250
GAK15	0-20	0, 10, 20
	30-50	30, 40, 50
	60-100	60, 80, 100
	500-1000	500, 750, 1000

Table 2. Rhizaria identification and biomass details. *ID characteristics:* identifying characteristics used to classify taxa. *Biovolume shape:* most appropriate 3D geometric shape assigned to each individual; corresponding volumetric equations are listed in Supplemental Table 1. *Average biovolume and range:* listed for each taxonomic group; individuals lacking nuclei were not included. * indicates taxa with all individuals included in biovolume and biomass analyses. *Carbon conversion factor:* most relevant carbon density value for each taxonomic group. *Reference:* source of the carbon conversion factor; CCE=California Coastal Ecosystem.

Taxonomic group	ID characteristics	Biovolume shape	Average biovolume (μm^3 +/- SD) and range (μm^3)	Carbon conversion factor (pg C μm^{-3})	Reference
Unknown Rhizaria #1-5 (Fig. 3a-d,f)	pseudopodia and/or skeleton	spheroid or prolate spheroid	8.5×10^5 (+/- 1.8×10^6) 1.3×10^4 – 4.1×10^6 n=5	0.0089	Nassellaria value from CCE (Laget et al. 2023)
Unknown Rhizaria #6 (Fig. 3e)	ovoid central capsule, large ovoid nucleus, DNA-free cellular compartment, and variable axopodia-like structures	prolate spheroid	1.92×10^4 (+/- 1.28×10^4) 4.44×10^3 – 7.65×10^4 n=66*		
Acantharia: Radiolaria: Retaria: Rhizaria	central capsule, ≤10 radial spicules, multiple nuclei in central capsule	spheroid	4×10^4 (+/- 3×10^5) 0.6×10^2 – 4×10^6 n=402	0.04	various Acantharia from Mediterranean Sea (Mansour et al. 2021)
Polycystina: Radiolaria: Retaria: Rhizaria	latticed skeleton, nucleus	prolate spheroid	5.0×10^5 n=1	0.0089	Nassellaria value from CCE (Laget et al. 2023)
Spumellaria: Polycystina: Radiolaria: Retaria: Rhizaria	2 concentric latticed spherical shells, <10 spicules, nucleus in inner shell	spheroid	1.320×10^4 (+/- 1.425×10^4) 1.704×10^3 – 5.063×10^4 n=18	0.2797	various Spumellaria from CCE (Laget et al. 2023)
Nassellaria: Polycystina: Radiolaria: Retaria: Rhizaria	asymmetrical or umbrella-shaped skeleton, variable # spines, nucleus in cephalis/thorax regions	cylinder, prolate spheroid, or spheroid	2.5×10^4 (+/- 2.7×10^4) 6.4×10^2 – 1.7×10^5 n=67	0.0089	*Phlebarachnium* sp. from CCE (Laget et al. 2023)
Collodaria: Polycystina: Radiolaria: Retaria: Rhizaria	large (>100 µm) multinucleated sphere	spheroid	6.71×10^5 (+/- 2.83×10^5) 1.23–9.86×10^5 n=8*	0.189	solitary *Thalassicolla* sp. from Mediterranean Sea (Mansour et al. 2021)

Sticholonche zanclea: *Sticholonche* sp.: Taxopodida: Sticholonchea: Radiolaria: Retaria: Rhizaria	≥3 oar-like axopodia and/or spicule bundles, ovoid to diamond-shaped central capsule with nucleus	prolate spheroid	5×10^4 ($+/- 2 \times 10^4$) $2–8 \times 10^4$ n=8	0.04	Acantharia value from Mediterranean Sea (Mansour et al. 2021)
Foraminifera: Retaria: Rhizaria	multiple connected globular chambers, dark brown, with/without spines, nucleus in each chamber	prolate spheroid	4.5×10^5 ($+/- 1.2 \times 10^6$) $0.19–9.0 \times 10^5$ n=112	0.061	*Globigerinoides ruber* from Bermuda (Michaels et al. 1995)
Challengeridae: Phaeodaria: Thecofilosea: Monadofilosa: Cercozoa: Rhizaria	ovoid/egg-shaped skeleton, oral spine, central capsule with dark brown/red phaeodium (multiple spherical compartments), large ovoid nucleus	prolate spheroid	4.85×10^3 ($+/- 1.40 \times 10^3$) $1.52–9.30 \times 10^3$ n=77	0.0397	*Protocystis* sp. from CCE (Laget et al. 2023)
Protocystis acornis: *Protocystis* spp.*:* Challengeridae: Phaeodaria: Thecofilosea: Monadofilosa: Cercozoa: Rhizaria	ovoid/egg-shaped skeleton, forked oral spine, central capsule with dark brown/red phaeodium, large ovoid nucleus	prolate spheroid	1.52×10^5 ($+/- 1.05 \times 10^5$) 7.57×10^4– 8.66×10^5 n=52*	0.0397	*Protocystis* sp. from CCE (Laget et al. 2023)

Results

Oceanographic setting

During Summer 2023 in the NGA, a pronounced density gradient was evident nearshore in the upper 30 m (GAK1, Figure 2a). The pycnocline was deeper farther offshore at GAK9 and GAK15 (~18-27 m, Figure 2a) compared to ~5 m on the inner to mid shelf (GAK1 and GAK5, Figure 2a). Salinity ranged from ~32.0 to 32.3 at the surface at GAK5, GAK9, and GAK15, with a prominent low-salinity, freshwater signature at GAK1 (~27.7, Figure 2b). Temperature at the surface increased with distance offshore and was lowest at GAK1 (9.5°C, Figure 2c). These cooler inshore temperatures and low salinities were likely influenced by coastal freshwater inputs transported westward by the Alaska Coastal Current (Figure 1). Nitrate was lowest at GAK1 and increased with distance along the Seward line (Figure 2d). At GAK1, GAK5, and GAK9, nitrate was <5.0 µM in the upper 20 m and ranged from 13.9 to 20.5 µM at 100 m (Figure 2d). The open ocean saw elevated nitrate levels compared to the shelf region, varying between 6.26 and 6.76 µM in the upper 20 m and ultimately reaching 27.3 µM at 100 m (GAK15, Figure 2d). Particulate matter likely in the form of glacial fluor, suspended sediments, and cells was evaluated. There were more particles nearshore as demonstrated by lower percent beam transmission in the upper 15 m and below 65 m at GAK1 (73 to <80% and 82 to <90%, respectively, Figure 2e). Biological indicators were also examined, including size-fractionated chlorophyll-a (large cells >20 µm and small cells <20 µm that represent potential Rhizaria algal prey and symbionts/commensals, respectively) and primary productivity. Large cell chlorophyll-a maxima were located between 10 and 30 m on the shelf (range 0.11-0.69 mg L^{-1}, GAK1-9, Figure 2f) and 40 m at GAK15 (0.22 mg L^{-1}, Figure 2f); the highest was at GAK1 (10 m, 0.69 mg L^{-1}, Figure 2f). Small cell chlorophyll-a maxima were at 10 m and similar in magnitude on shelf stations (range 0.87-0.90 mg L^{-1}, GAK1-9, Figure 2g), whereas offshore it was greatest at 30-40 m (0.29-0.30 mg L^{-1}, GAK15, Figure 2g). Integrated primary production across Seward line stations GAK1, GAK5, GAK9, and GAK15 averaged 935.5 mg C m^{-2} d^{-1} (Figure 2h) and was greatest inshore (1,069 mg C m^{-2} d^{-1}, GAK1, Figure 2h). Picophytoplankton contributed over

50% of primary production at GAK5 and GAK9 (<3 µm, 447 and 481 mg C m^{-2} d^{-1}, respectively, Figure 2h).

Rhizaria diversity

Ten taxonomic groups were classified in this study (Table 2). As described in Methods, Rhizarians were assigned to the lowest taxonomic classification possible based solely on morphology as visualized through an inverted epi-fluorescence microscope. Some individuals exhibited Rhizaria characteristics but were unidentifiable and therefore could only be classified as "Unknown Rhizaria", of which there were six species/morphotypes (Figure 3). One Unknown Rhizaria morphotype did not closely resemble any organism in the literature but was abundant in the NGA (Unknown Rhizaria #6, Figure 3e; max abundance 6.4 cells L^{-1}, Table 3). Rhizaria cells ranged in volume from 0.6 x 10^2 μm^3 (Acantharia) to 9.0 x 10^5 μm^3 (Foraminifera) (Table 2). Acantharia sizes were variable, ranging from 0.6 x 10^2 to 4 x 10^6 μm^3 (Table 2) and occurred in 20 different morphotypes (Figure 4a-t). These Radiolarians were multinucleated as seen previously by Suzuki et al. (2009). Individuals from the single-species order Taxopodida (*Sticholonche zanclea*) (Figure 5a) varied between 2–8 x 10^4 μm^3 (Table 2). Nassellaria exhibited the greatest morphological diversity of the Polycystines, with 24 morphotypes (Figure 6e-z, iii-iv) that ranged in size from 6.4 x 10^2–1.7 x 10^5 μm^3 (Table 2). Four Spumellaria (Figure 6a-d), one Collodaria (Figure 6ii), and two Unknown Polycystine (Figure 6v-vi) morphotypes were also identified. Five morphotypes of Foraminiferans were categorized based on general size (small, large, very large) and presence/absence of spines (Figure 7a-e). These multichambered, globular protists were by far the largest Rhizarians observed and varied in size from 0.19-9.0 x 10^5 μm^3 (Table 2). Four morphotypes of Challengeridae were found (Figure 8a-d), including individuals that displayed *Protocystis acornis* characteristics, mainly a forked oral spine (Figure 8d). Challengeridae (including *P. acornis*) volumes varied between 1.52 x 10^3 and 8.66 x 10^5 μm^3 (Table 2).

Rhizaria ecology

Distributions and community composition

In Summer 2023, Rhizaria abundances generally increased with depth and with distance offshore. On the inner shelf at GAK1 and GAK5, abundances were greatest in the deep water (<1.0 and 10 cells L^{-1}, respectively, Figure 9a). Abundances reached their depth maxima in intermediate waters both on the outer shelf and in the open ocean (GAK9 and GAK15, 25 and 19 cells L^{-1}, respectively, Figure 9a). Across the NGA, Rhizaria abundances were generally lowest at the surface, ranging from 0 to 4 cells L^{-1} (Figure 9a). In fact, no Rhizarians were detected at the nearshore GAK1 surface and mid depths. At GAK9 and GAK15, deep-water abundances diminished at least twofold relative to the intermediate water quantities. In contrast to abundance, Rhizaria biomass did not show distinct cross-shelf or vertical patterns, since each station had different depth maxima (Figure 9b). At GAK5, biomass peaked at the surface (105 ng C L^{-1}, Figure 9b) which was influenced by large Foraminiferans (Foraminifera 100 ng C L^{-1}, Table 4). At GAK9, biomass was highest in the deep water (143 ng C L^{-1}, Figure 9b) which was influenced by Collodarians (115 ng C L^{-1}, Table 4). Off the shelf at GAK15, biomass was greatest at mid depths (137 ng C L^{-1}, Figure 9b).

Acantharia was the most abundant taxon in the NGA followed by Foraminifera, which were about threefold less abundant (Figure 9c,d). Similar to the Rhizaria cross-shelf gradient, Acantharia and Foraminifera generally increased with distance offshore, while the vertical distributions exhibited opposite trends. Acantharia were more likely to be found below the surface, peaking at intermediate and deep depths, depending on the location (maximum abundance 12 cells L^{-1} at GAK15 intermediate waters, Figure 9c). In contrast, most Foraminifera resided at the surface and mid waters, reaching 4.1 cells L^{-1} at GAK15 (Figure 9d).

Rhizaria community composition was evaluated in terms of the three phyla (Cercozoa, Foraminifera, and Radiolaria) and by Radiolaria subgroup since it was the most diverse phylum. Foraminifera was consistently the dominant phylum in surface waters extending from the mid-shelf (GAK5) to the open ocean (GAK15) (82 to 92% relative abundance, Figure 10a). The exception was

GAK1, which did not have any Rhizarians at the surface and mid depths. Foraminifera was the only phylum present at GAK1 intermediate depths (100% relative abundance, Figure 10a). At all stations, Foraminifera influenced Rhizaria biomass to the greatest extent at 0-20 m and 30-50 m depths (73 to 100% relative biomass, Figure 10b) due to their large sizes. Due to the high Acantharia abundances, Radiolaria was the most abundant phylum across the NGA with >50% relative abundance at all station depths below the surface, excluding GAK1 60-80 m where the community was made up exclusively by Foraminifera (Figure 10a). Acantharia comprised >60% of the Radiolarian community at all station depths except GAK5 30-50 m where they were absent (Figure 10c). Nassellaria was the second most abundant Radiolarian (range 3.4 to 36% relative abundance, Figure 10c) followed by Spumellaria (range 2.0 to 57% relative abundance, Figure 10c). Acantharia also dominated the Radiolarian biomass at most depths and locations (>70% relative biomass, Figure 10c) except for discrete samples GAK5 30-50 m, 60-80 m and GAK15 100-250 m where Spumellaria, Nassellaria, and Collodaria contributed higher biomass, respectively. Cercozoa was the least abundant phylum overall; this group contributed anywhere from 2.4 to 37% relative abundance (Figure 10a) and was more likely to reside in intermediate and deep waters. This phylum comprised the majority of Rhizarian biomass at GAK5 90-150 m and GAK9 60-80 m (79 and 65% relative biomass, respectively, Figure 10b) where Radiolaria dominated in terms of abundance. Cercozoa was more prominent than Radiolaria at the aforementioned locations in terms of relative biomass because *P. acornis* individuals were on average roughly one order of magnitude larger than Acantharia (1.52×10^5 and 4×10^4 μm^3, respectively, Table 2).

NGA Rhizaria communities were more clearly separated by depth than by station as demonstrated by nMDS analysis. Surface communities were distinct from many of the deeper communities as seen by the isolation of surface samples along NMDS1 and some separation along NMDS2 (Figure 11). Surface communities were similar between stations as seen by their adjacent locations along both axes. In contrast, the mid, intermediate, and deep communities were not clearly separated. In general, Rhizaria communities were not obviously separated by station because they did not exhibit unique locations in ordination space.

Trophic interactions

The proportion of Rhizarians with captured prey generally increased with distance offshore and declined with depth (Figure 12a). The highest proportions of Rhizaria with captured prey were observed far offshore at GAK15. Notably, incidences of prey capture were not observed nearshore (GAK1). On the mid to outer shelf, the proportion of Rhizarians with captured prey was greatest at the surface (GAK5 and GAK9, 25% and 28%, respectively, Figure 12a). Off the shelf, prey capture was a bit more common in intermediate waters (GAK15, 33%, Figure 12a) but was still elevated at the surface and mid depths (31% and 25%, respectively, Figure 12a). The percentage of Rhizarians with prey captured reached a depth minimum in the deep waters at GAK15 (3.0%, Figure 12a). Low prey capture (<10%) was also evident in the intermediate and deep waters at GAK5 and GAK9 (range 7.6 to 9.1%, Figure 12a), as well as at mid depths at GAK5 (8.0%, Figure 12a).

Most taxonomic groups identified in this study had individuals that exhibited prey capture. The proportion of individuals from a particular taxon with captured prey varied between 1.7% and 33% across the Seward line, although the majority of incidences at each station were >13% (Figure 12c). The taxon with a consistently elevated proportion of individuals with prey captured at each station (minus GAK1, which had no incidences of prey capture) was Foraminifera (range 20 to 30%, Figure 12c). Foraminifera and Acantharia had similar prey capture frequency trends across the Seward line. The highest proportions of Foraminiferans and Acantharians with captured prey occurred in the open ocean at GAK15 (30% and 32%, respectively, Figure 12c) and decreased with proximity to shore. The Challengeridae family exhibited similar prey capture proportions to Foraminifera and Acantharia at GAK5 (17% compared to 20% and 8.5%, respectively, Figure 12c) and GAK15 (24% compared to 30 and 32%, respectively, Figure 12c). Unknown Rhizarians with captured prey were observed on the outer shelf and open ocean (GAK9 and GAK15, 1.7% and 22%, respectively, Figure 12c). Individuals belonging to the Spumellaria, Nassellaria, and Taxopodida groups had incidences of prey capture at only one offshore station each, either GAK9 or GAK15; these ranged between 14 and 33% (Figure 12c). The proportion of Taxopodida (*Sticholonche zanclea*) with prey captured at GAK15 was the highest observed out of all taxonomic

groups (33%, Figure 12c), although these organisms were some of the least abundant (Seward line total abundance 1.0 cell L^{-1}, Table 3). Diatoms (*Chaetoceros* spp., *Corethron* spp., *Melosirales* spp., and *Thalassiosira* spp.) were the most common prey item followed by cells of unknown identity (37 and 32% of prey captures, respectively, Figure 12e). Other types of prey were unidentified fluorescent algal cells, ciliates including tintinnids, copepod eggs, unknown Rhizarians, silicoflagellates, nauplii, and dinoflagellates (*Protoperidinium* spp.). Epi-fluorescence images of captured prey are shown in Figures 4b,c,f,g,m, 6z, 7b,c and 8d.

The proportion of Rhizarians that associated with algal cells generally increased with distance offshore and decreased with depth (Figure 12b). Fewer than 30% of Rhizarians were found interacting with algal cells at each station depth (Figure 12b). Associations with algae occurred at all stations except on the inner shelf at GAK1. The highest incidences were at the surface on the mid (GAK5) and outer (GAK9) shelf and at mid depths in the open ocean (GAK15) (14%, 22%, and 22%, respectively, Figure 12b), while the lowest incidences were in deep waters at GAK5 and GAK9 (2.2% and 1.0%, respectively, Figure 12b). At GAK15, Rhizaria-algal cell interactions did not occur in the deep waters, while at GAK9 this was true at intermediate depths.

Four out of ten taxa exhibited interactions with algal cells: Foraminifera, Acantharia, Nassellaria, and Unknown Rhizaria. Epi-fluorescence images of associated algae are shown in Figures 3f, 4d,h and 7a,d,e. Foraminifera had the highest proportions of individuals with algal cell associations (GAK5 to GAK15, range 11 to 17%, Figure 12d) followed by Acantharia (GAK5 to GAK15, range 2.0 to 12%, Figure 12d). Incidences of algal cell associations in Foraminifera and Acantharia demonstrated opposite cross-shelf trends. Proportions of Foraminifera with algal cell associations decreased with distance offshore while proportions of Acantharia that interacted with algae generally increased with distance offshore (Figure 12d). Nassellarians that associated with algae were only present at GAK5 but exhibited a similar incidence to Acantharia there (6.3% compared to 3.7%, respectively, Figure 12d). One Unknown Rhizaria individual interacted with algal cells (Figure 3f), or 25% of individuals at GAK5 (Figure 12d).

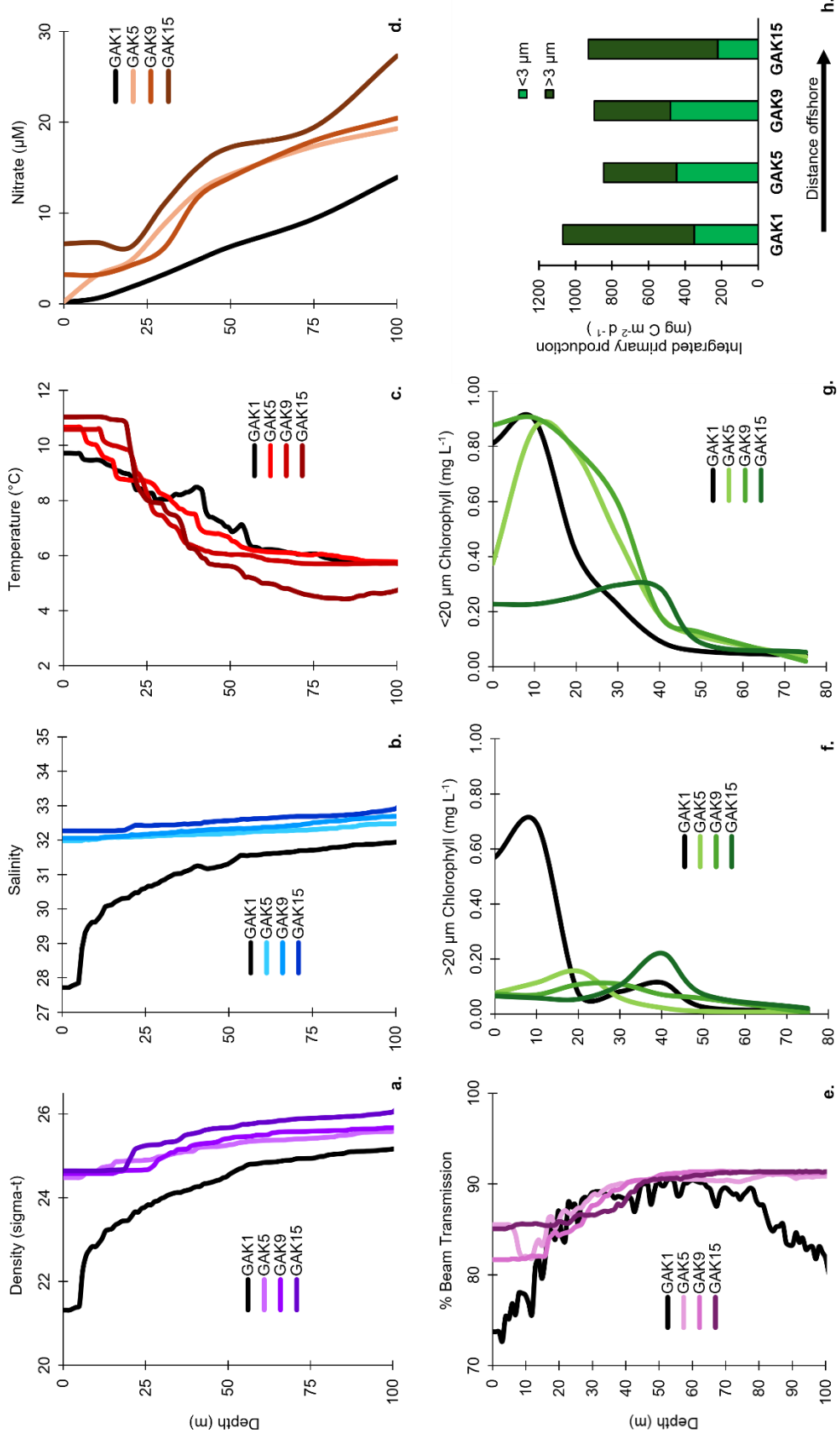

Figure 2. Vertical profiles of oceanographic parameters and cross-shelf primary productivity at GAK1, GAK5, GAK9, and GAK15 in summer 2023. a) density (sigma-theta) at 0-100 m, **b)** salinity at 0-100 m, **c)** temperature (°C) at 0-100 m, **d)** nitrate (µM) at 0-100 m, **e)** beam transmission (%) at 0-100 m, **f)** >20 µm chlorophyll-a (µg L^{-1}) at 0-75 m, **g)** <20 µm chlorophyll-a (µg L^{-1}) at 0-75 m, and **h)** integrated primary productivity (mg C m^2 d^{-1}) from cells separated into <3 µm and >3 µm size-fractions.

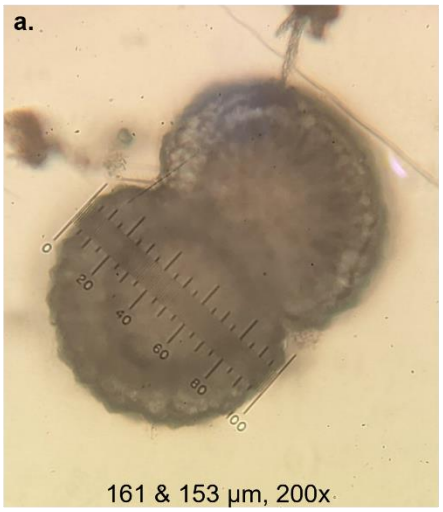

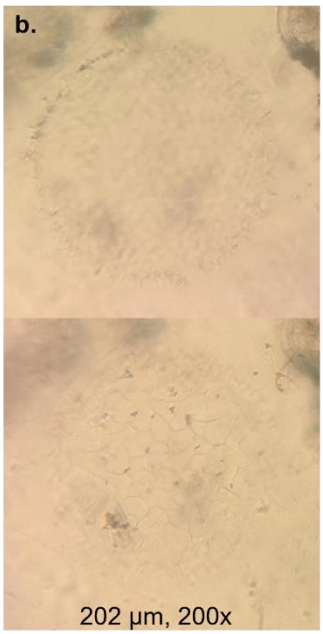

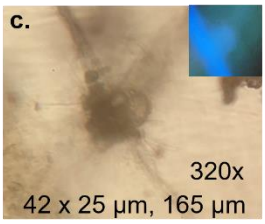

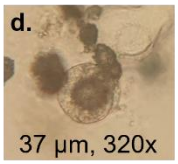

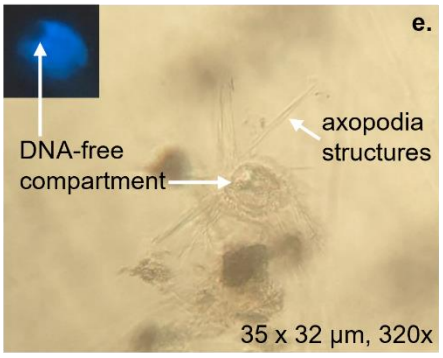

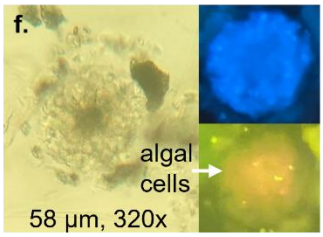

Figure 3. Unknown Rhizaria diversity. Dimensions of the central capsule(s) used in biovolume calculations, spicule extent length (**d** and **f**), and magnification are noted. Inset images using UV and blue light illumination show DAPI-stained nuclei and fluorescent photopigments, respectively. **a)** two large cells with scalloped outer boundaries. **b)** two views of a large, empty, latticed sphere with short spines. **c)** irregular shaped cell with spherical endoplasm and at least 8 spines. **d)** small sphere with large, dense endoplasm. **e) Unknown Rhizaria #6:** cell with an ovoid central capsule, a large ovoid nucleus, a DNA-free compartment, and variable axopodia-like structures. **f)** small sphere with small dense endoplasm and at least 4 spines.

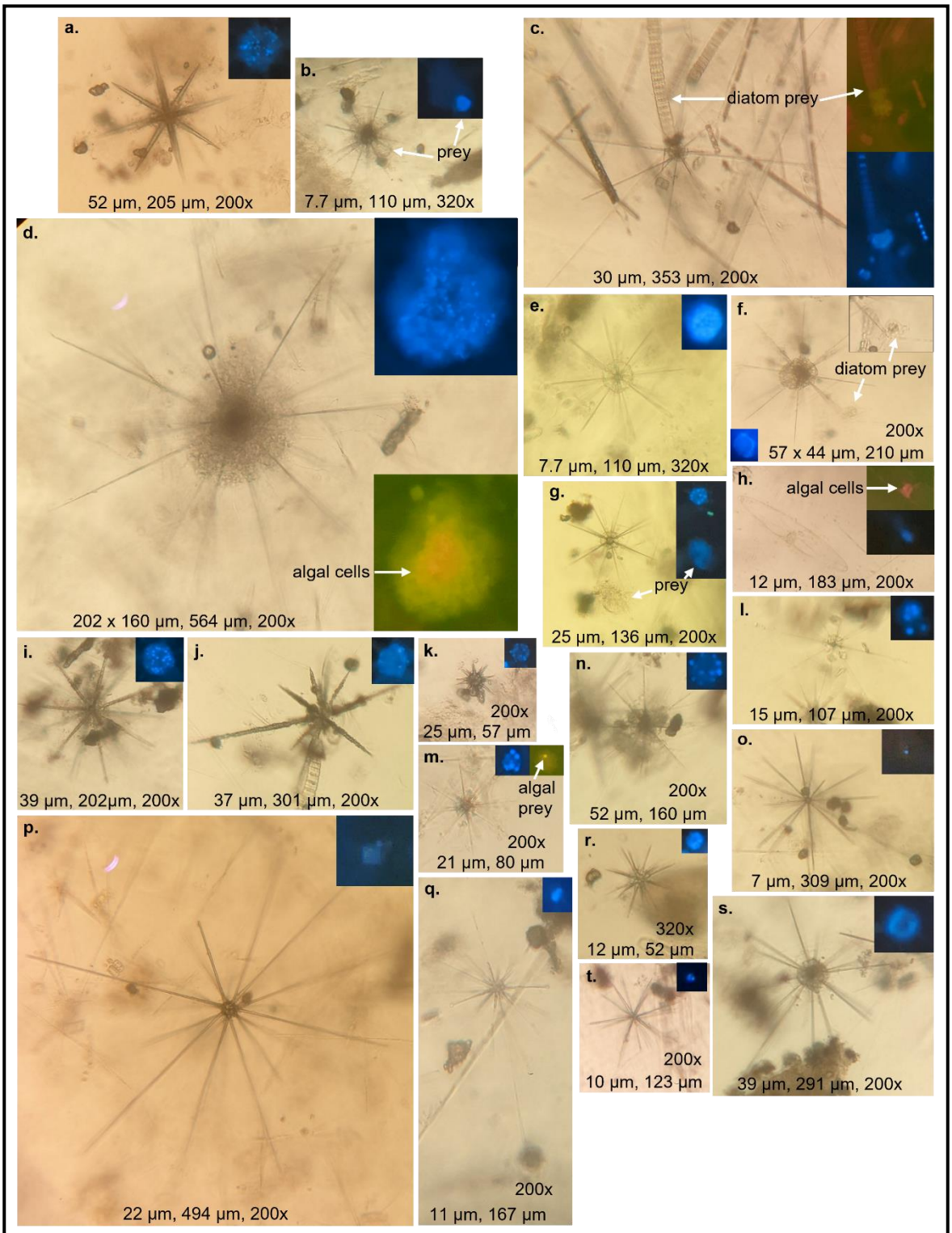

Figure 4. Acantharia diversity. Dimensions of the central capsule used in biovolume calculations, spicule extent length, and magnification are noted. Inset images using UV and blue light illumination show DAPI-stained nuclei and fluorescent photopigments, respectively. **a-t)** Acantharia morphotypes: **b)** and **g)** with captured unknown prey containing nuclei, **c)** and **f)** with captured diatom prey, **d)** and **h)** with intracapsulum-associated red-orange and red algal cells, and **m)** with algal prey in endoplasm.

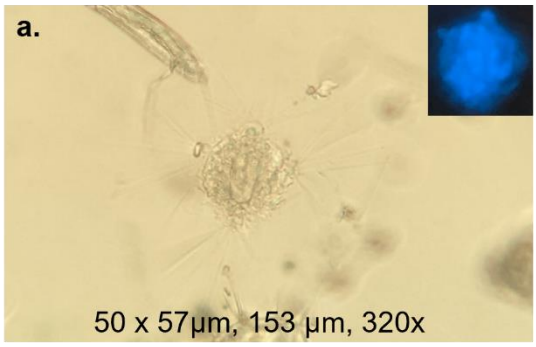

Figure 5. Taxopodida diversity. Dimensions of the central capsule used in biovolume calculations, spicule extent length, and magnification are noted. Inset images using UV and blue light illumination show DAPI-stained nuclei and fluorescent photopigments, respectively. **a)** *Sticholonche zanclea*.

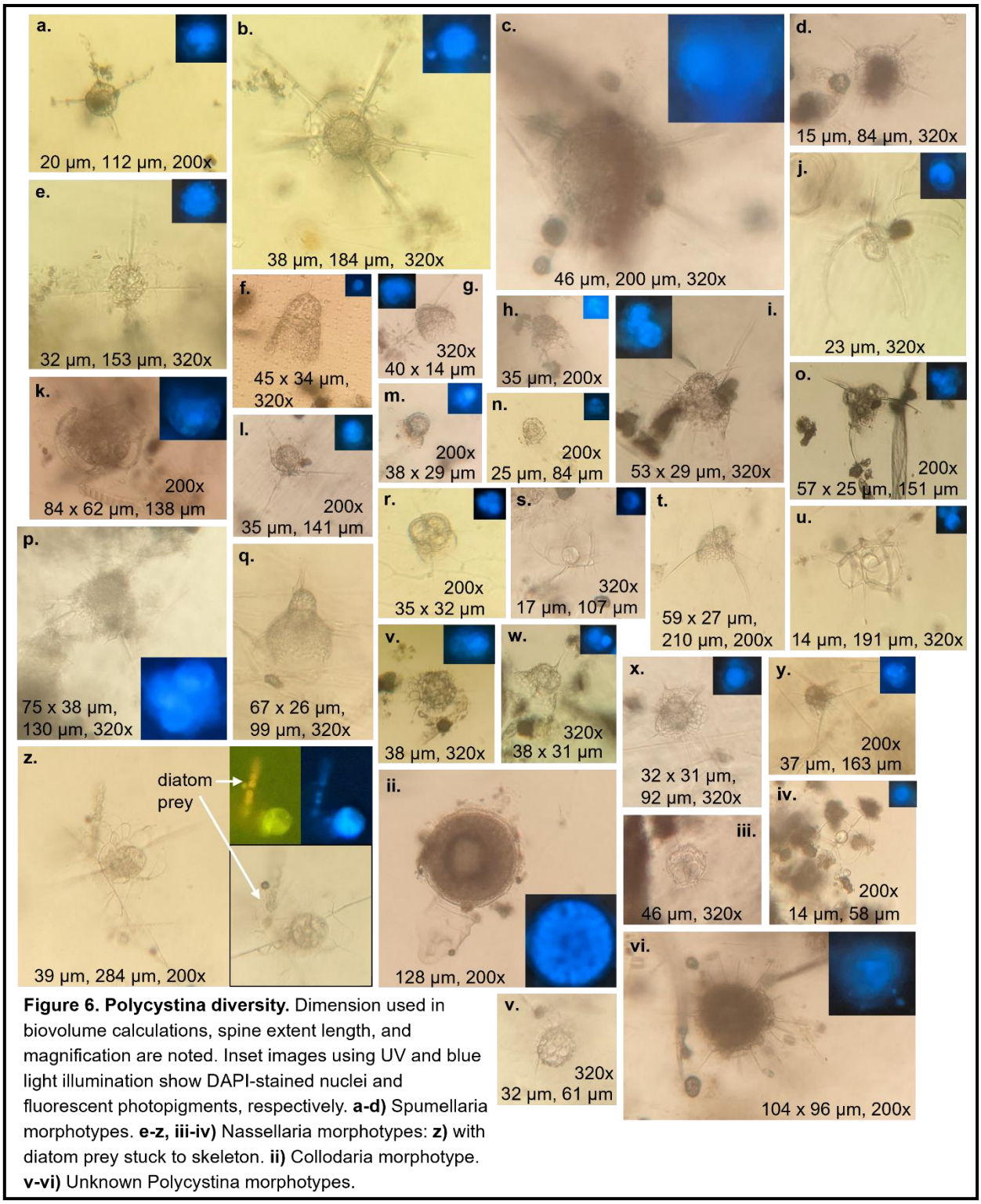

Figure 6. Polycystina diversity. Dimension used in biovolume calculations, spine extent length, and magnification are noted. Inset images using UV and blue light illumination show DAPI-stained nuclei and fluorescent photopigments, respectively. **a-d)** Spumellaria morphotypes. **e-z, iii-iv)** Nassellaria morphotypes: **z)** with diatom prey stuck to skeleton. **ii)** Collodaria morphotype. **v-vi)** Unknown Polycystina morphotypes.

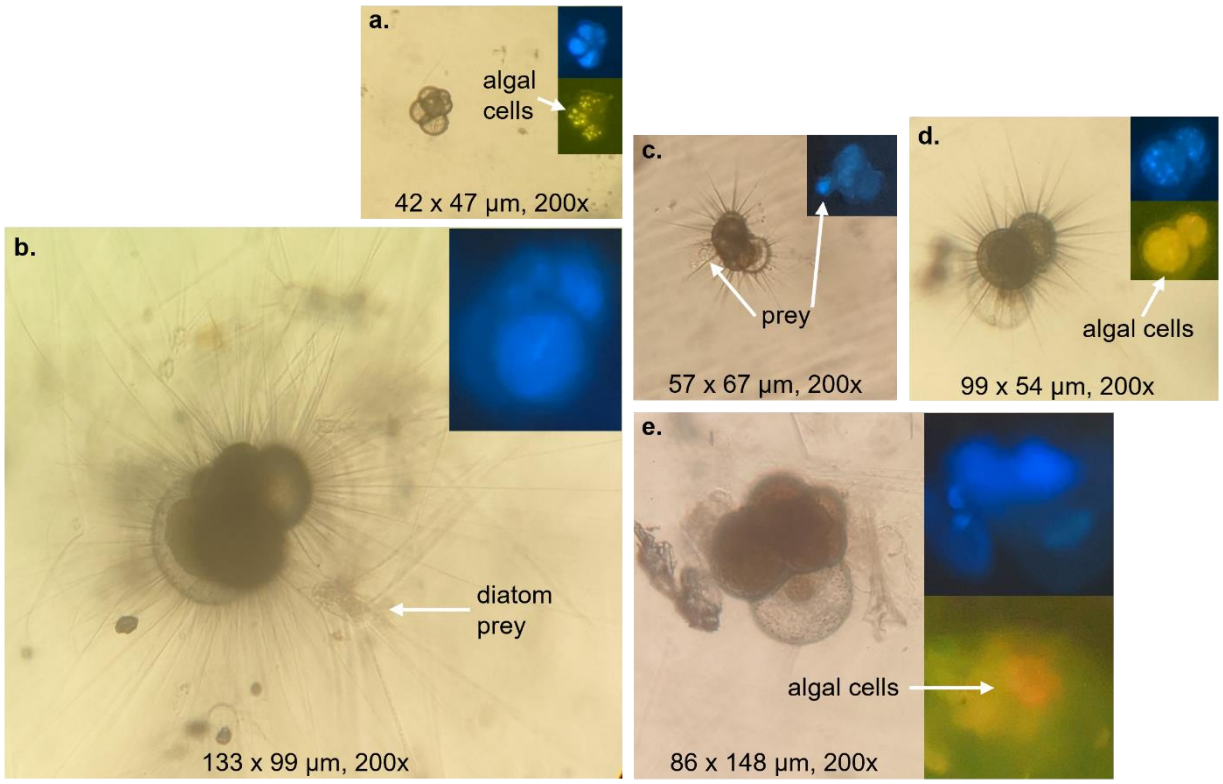

Figure 7. Foraminifera diversity. Dimensions used in biovolume calculations and magnification are noted. Inset images using UV and blue light illumination show DAPI-stained nuclei and fluorescent photopigments, respectively. **a-e)** Foraminifera morphotypes: **a)** small (<90 µm), non-spinose (note intrashell-associated yellow algal cells in this individual), **b)** very large (>130 µm), spinose; *Chaetoceros* spp. prey captured in spines, **c)** small (<90 µm), spinose; unknown prey captured in spines and to chamber, **d)** large (>90 µm), spinose (note intrashell-associated golden-yellow algal cells in this individual), and **e)** large (>90 µm), non-spinose (note intrashell-associated red-orange algal cells in this individual).

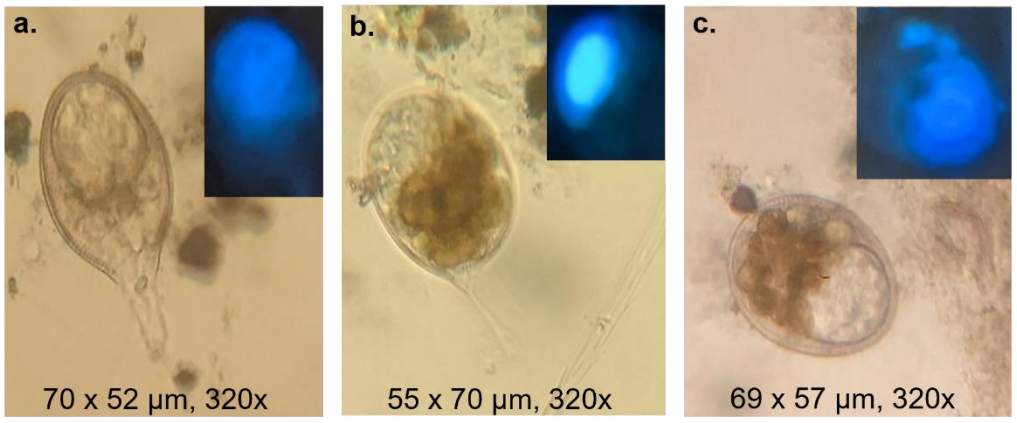

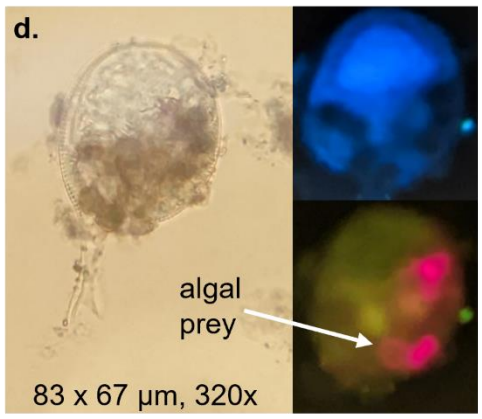

Figure 8. Cercozoa diversity. Dimensions used in biovolume calculations and magnification are noted. Inset images using UV and blue light illumination show DAPI-stained nuclei and fluorescent photopigments, respectively. **a-c)** Challengeridae morphotypes: **a)** with a pointed oral spine, **b)** with an oral spine of uncertain shape, and **c)** no oral spine seen. **d)** *Protocystis acornis* with digested algal prey in phaeodium.

Table 3. Detailed abundance data at station depths for each taxonomic group in cells L^{-1} with (# observed).

	GAK1 0-20 m	GAK1 30-50 m	GAK1 60-80 m	GAK1 100-250 m	GAK5 0-20 m	GAK5 30-50 m	GAK5 60-80 m	GAK5 90-150 m	GAK9 0-20 m	GAK9 30-50 m	GAK9 60-80 m	GAK9 100-250 m	GAK15 0-20 m	GAK15 30-50 m	GAK15 60-100 m	GAK15 500-1000 m	Total
Unknown Rhizaria #1-5	0 (0)	0 (0)	0 (0)	0 (0)	0 (0)	0.45 (4)	0 (0)	0 (0)	0 (0)	0 (0)	0.11 (1)	0.11 (1)	0 (0)	0 (0)	0.11 (1)	0 (0)	0.78 (7)
Unknown Rhizaria #6	0 (0)	0 (0)	0 (0)	0 (0)	0 (0)	0 (0)	0 (0)	0 (0)	0 (0)	0.23 (2)	6.4 (56)	0 (0)	0 (0)	0 (0)	0.68 (6)	0.23 (2)	7.5 (66)
Acantharia	0 (0)	0 (0)	0 (0)	0.70 (6)	0.60 (5)	0 (0)	3.4 (30)	5.3 (47)	0.10 (1)	5.8 (51)	11 (100)	5.2 (46)	0.30 (3)	1.4 (12)	12 (109)	2.4 (21)	49 (431)
Polycystina	0 (0)	0 (0)	0 (0)	0 (0)	0 (0)	0 (0)	0 (0)	0 (0)	0 (0)	0 (0)	0 (0)	0 (0)	0 (0)	0.11 (1)	0 (0)	0.11 (1)	0.23 (2)
Spumellaria	0 (0)	0 (0)	0 (0)	0 (0)	0 (0)	0.90 (8)	0.40 (4)	0.10 (1)	0 (0)	0.40 (4)	0.20 (2)	0 (0)	0 (0)	0 (0)	0 (0)	0 (0)	2.2 (19)
Nassellaria	0 (0)	0 (0)	0 (0)	0 (0)	0 (0)	0.60 (5)	0.60 (5)	0.70 (6)	0 (0)	0.20 (2)	1.5 (13)	1.0 (12)	0 (0)	0.70 (6)	2.5 (22)	1.0 (9)	9.1 (80)
Collodaria	0 (0)	0 (0)	0 (0)	0 (0)	0 (0)	0 (0)	0 (0)	0 (0)	0 (0)	0 (0)	0 (0)	0.90 (8)	0 (0)	0 (0)	0 (0)	0 (0)	0.91 (8)
Sticholonche zanclea	0 (0)	0 (0)	0 (0)	0 (0)	0 (0)	0.10 (1)	0 (0)	0.10 (1)	0 (0)	0.20 (2)	0 (0)	0.20 (2)	0 (0)	0 (0)	0.34 (3)	0 (0)	1.0 (9)
Foraminifera	0 (0)	0 (0)	0.23 (2)	0 (0)	2.6 (23)	0.79 (7)	0.34 (3)	0.23 (2)	1.8 (16)	2.5 (22)	0.57 (5)	0.45 (4)	4.1 (36)	1.9 (17)	0.34 (3)	0 (0)	16 (140)
Challengeridae	0 (0)	0 (0)	0 (0)	0 (0)	0 (0)	0 (0)	0.23 (2)	2.5 (22)	0.10 (1)	0.23 (2)	3.1 (27)	1.6 (14)	0 (0)	0 (0)	1.7 (15)	0 (0)	9.4 (83)
Protocystis acornis	0 (0)	0 (0)	0 (0)	0 (0)	0 (0)	0 (0)	0 (0)	1.2 (11)	0 (0)	0 (0)	1.9 (17)	2.0 (18)	0 (0)	0 (0)	0.68 (6)	0 (0)	5.9 (52)

Table 4. Detailed biomass data at station depths for each taxonomic group in ng C L^{-1} with (sample size).

	GAK1 0-20 m	GAK1 30-50 m	GAK1 60-80 m	GAK1 100-250 m	GAK5 0-20 m	GAK5 30-50 m	GAK5 60-80 m	GAK5 90-150 m	GAK9 0-20 m	GAK9 30-50 m	GAK9 60-80 m	GAK9 100-250 m	GAK15 0-20 m	GAK15 30-50 m	GAK15 60-100 m	GAK15 500-1000 m	Total
Unknown Rhizaria #1-5	0 (0)	0 (0)	0 (0)	0 (0)	0 (0)	0.19 (4)	0 (0)	0 (0)	0 (0)	0 (0)	0.026 (1)	4.1 (1)	0 (0)	0 (0)	0.014 (1)	0 (0)	4.3 (7)
Unknown Rhizaria #6	0 (0)	0 (0)	0 (0)	0 (0)	0 (0)	0 (0)	0 (0)	0 (0)	0 (0)	0.041 (2)	1.1 (56)	0 (0)	0 (0)	0 (0)	0.086 (6)	0.15 (2)	1.4 (66)
Acantharia	0 (0)	0 (0)	0 (0)	0.4 (6)	2 (5)	0 (0)	4 (29)	3 (42)	0.4 (1)	5 (47)	8 (91)	2 (45)	0.07 (3)	40 (11)	20 (108)	0.6 (15)	85 (402)
Polycystina	0 (0)	0 (0)	0 (0)	0 (0)	0 (0)	0 (0)	0 (0)	0 (0)	0 (0)	0 (0)	0 (0)	0 (0)	0 (0)	0.51 (1)	0 (0)	0 (0)	0.51 (1)
Spumellaria	0 (0)	0 (0)	0 (0)	0 (0)	0 (0)	2.533 (8)	2.145 (4)	0.2411 (1)	0 (0)	1.869 (3)	0.7521 (2)	0 (0)	0 (0)	0 (0)	0 (0)	0 (0)	7.539 (18)
Nassellaria	0 (0)	0 (0)	0 (0)	0 (0)	0 (0)	0.11 (4)	9.3 (4)	0.15 (4)	0 (0)	0.036 (2)	0.28 (11)	0.18 (11)	0 (0)	0.069 (5)	0.57 (20)	0.091 (6)	11 (67)
Collodaria	0 (0)	0 (0)	0 (0)	0 (0)	0 (0)	0 (0)	0 (0)	0 (0)	0 (0)	0 (0)	0 (0)	115 (8)	0 (0)	0 (0)	0 (0)	0 (0)	115 (8)
Sticholonche zanclea	0 (0)	0 (0)	0 (0)	0 (0)	0 (0)	0.2 (1)	0 (0)	0.3 (1)	0 (0)	5 (1)	0 (0)	0.6 (2)	0 (0)	0 (0)	0.7 (3)	0 (0)	7 (8)
Foraminifera	0 (0)	0 (0)	0.36 (1)	0 (0)	100 (9)	14 (7)	0.81 (2)	0.84 (1)	16 (11)	45 (20)	1.6 (4)	1.5 (3)	68 (35)	100 (17)	0.74 (2)	0 (0)	350 (112)
Challengeridae	0 (0)	0 (0)	0 (0)	0 (0)	0 (0)	0 (0)	1.27 (2)	11.4 (21)	0.721 (1)	1.08 (2)	12.9 (26)	4.94 (10)	0 (0)	0 (0)	10.5 (15)	0 (0)	42.8 (77)
Protocystis acornis	0 (0)	0 (0)	0 (0)	0 (0)	0 (0)	0 (0)	0 (0)	7.21 (11)	0 (0)	0 (0)	9.67 (17)	14.6 (18)	0 (0)	0 (0)	4.26 (6)	0 (0)	35.7 (52)

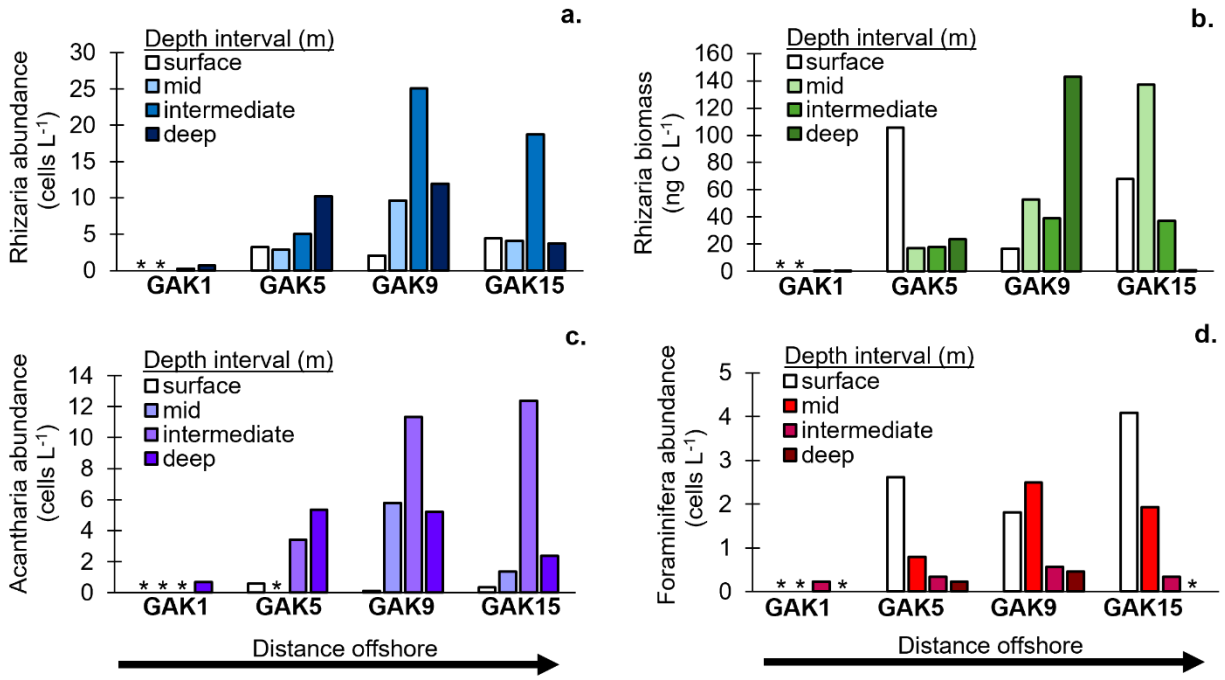

Figure 9. Distributions of **a)** Rhizaria abundance (cells L^{-1}) (n=897), **b)** Rhizaria biomass (ng C L^{-1}) (n=819), **c)** Acantharia abundance (cells L^{-1}) (n=431) and **d)** Foraminifera abundance (cells L^{-1}) (n=140) at different depths across the Seward line. Depth intervals are shown in Table 1. * = none detected.

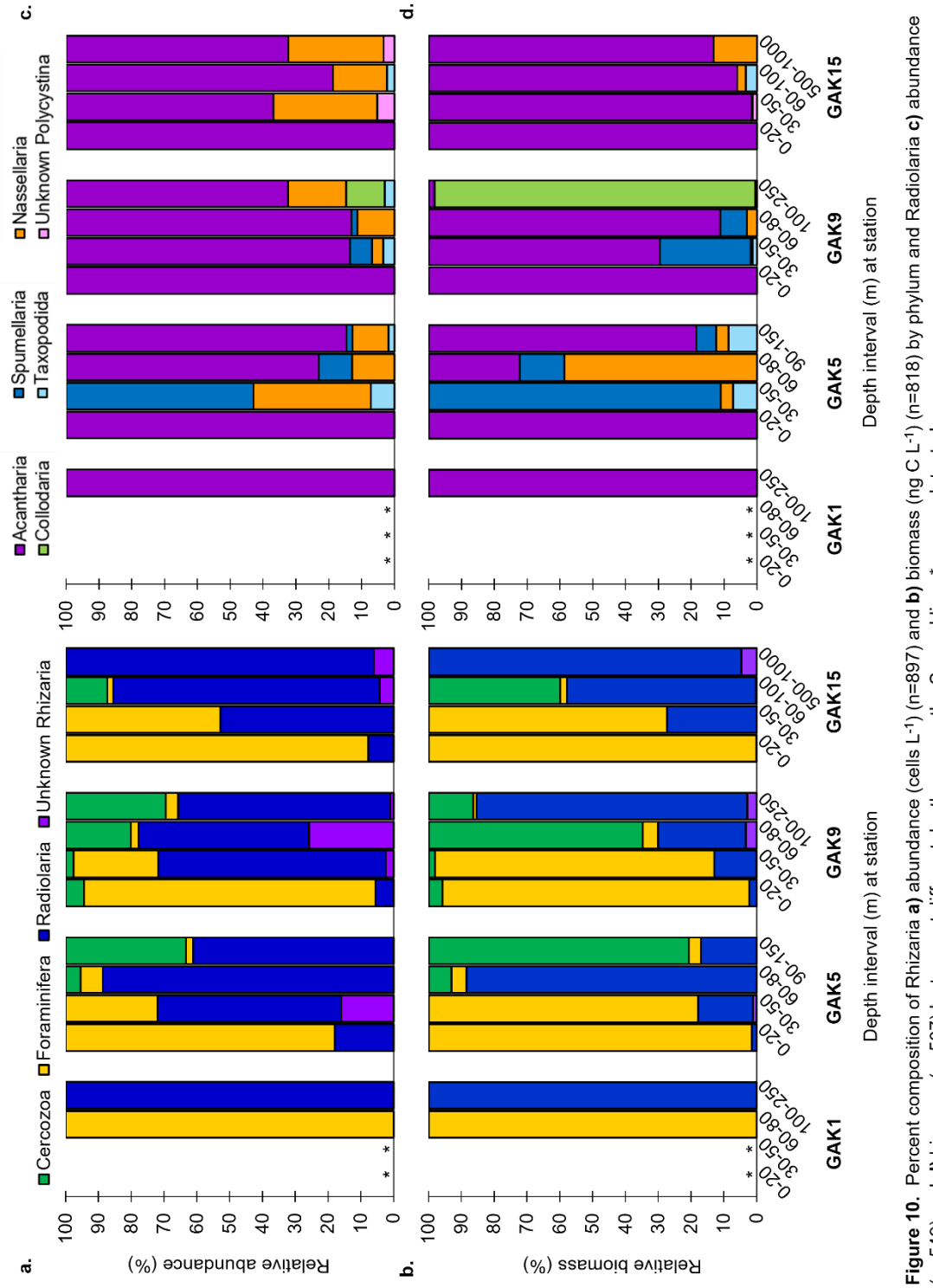

Figure 10. Percent composition of Rhizaria **a)** abundance (cells L^{-1}) (n=897) and **b)** biomass (ng C L^{-1}) (n=818) by phylum and Radiolaria **c)** abundance (n=549) and **d)** biomass (n=507) by taxon at different depths across the Seward line. * = none detected.

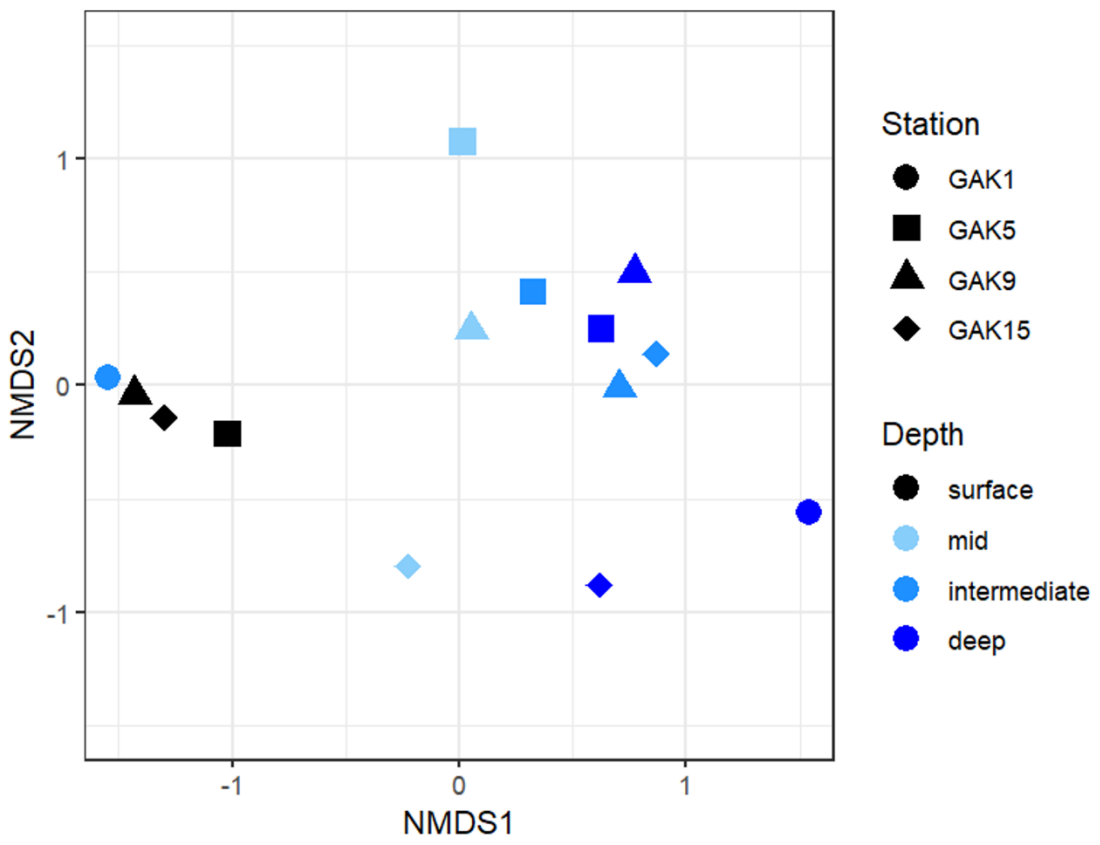

Figure 11. Relationship between Rhizaria communities at different station depths in ordination space.

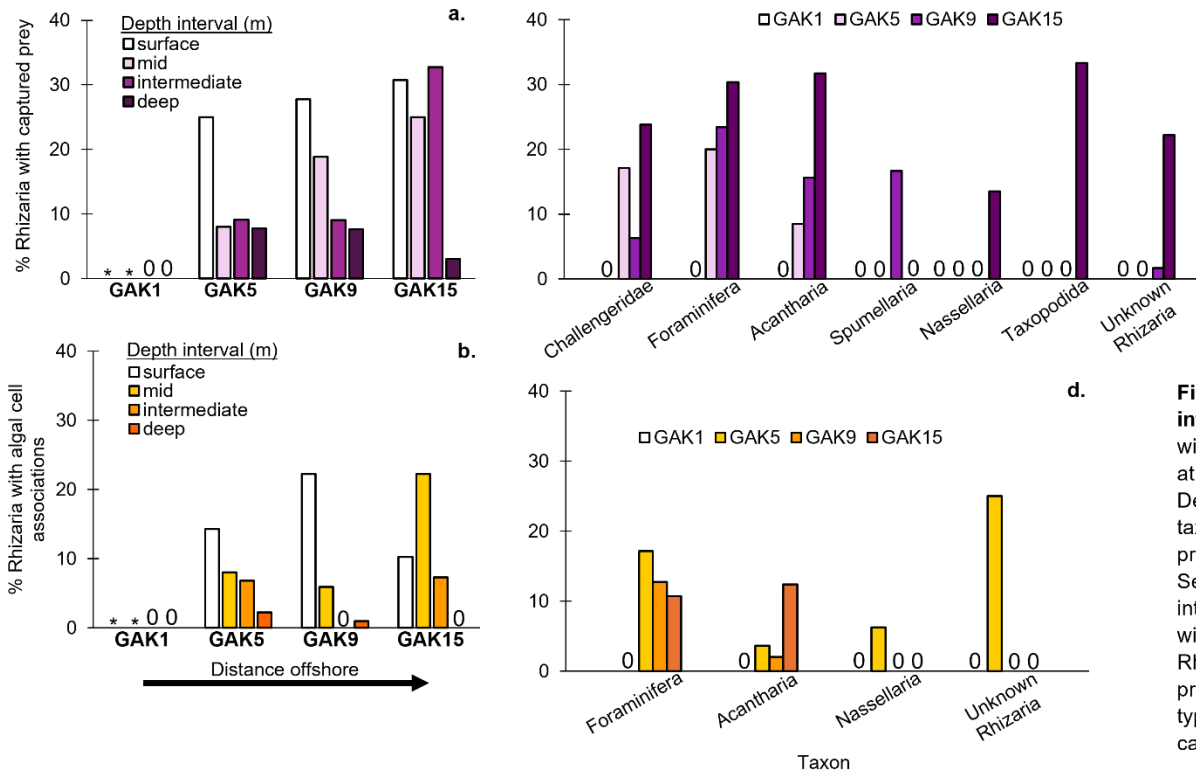

e.

Prey type	% Prey captures
Diatom	37
Unknown cell	32
Unknown algal cell	18
Ciliate	7.6
Egg	4.8
Unknown Rhizaria	3.4
Silicoflagellate	2.1
Nauplii	1.4
Dinoflagellate	0.69

Figure 12. Summary of Rhizaria trophic interactions in the NGA. Distributions of % Rhizaria with **a)** captured prey and **b)** algal cell associations at different depths across the Seward line (n=897). Depth intervals are outlined in Table 1. Grouped by taxon, distributions of % Rhizaria with **c)** captured prey and **d)** algal cell associations across the Seward line (n=897). Taxa that lacked such interactions were not included. Total # of individuals with captured prey = 145 and with algae = 45. * = no Rhizaria detected; 0 = no individuals with captured prey (a and c) or algae (b and d). **e)** Table of prey types and the proportion each was involved in a prey capture event (n=155).

Discussion

Our study presents the first quantitative depiction of living planktic Rhizaria ecology in the eastern subarctic Pacific Ocean. We report some of the highest Rhizaria abundances from any ocean environment to date; peak abundance in the NGA was 25 cells L^{-1}. Therefore, we suggest a revision to the current biogeographical paradigm, which posits that abundances are highest at the equator and decrease towards the poles (Casey 1966, 1971, Petrushevskaya 1971, Renz 1976, Be 1977, Boltovskoy and Correa 2017). In the NGA, Rhizaria were more likely to be found farther from shore. The phyla exhibited clear vertical depth niches: Foraminifera preferred to live near the surface, Radiolaria were widespread, and Cercozoa favored deep waters. Acantharia was a morphologically diverse, cosmopolitan group that dominated the Rhizaria community. An abundant new species was discovered that was deemed an Unknown Rhizarian, but we welcome other interpretations from fellow Rhizaria experts. Our data supports the current knowledge that Rhizaria are predators of common meso- and microzooplankton like diatoms and ciliates and hosts to symbiotic/commensal algal cells. At the same time, this research improved our understanding of the unique role that Rhizaria play in food web dynamics with one of the first detailed accounts of *in situ* predator-prey interactions and algal cell associations and how the prevalence of these trophic activities is related to the physical environment. We demonstrated that the frequencies of both prey capture and algal association were generally higher near the surface and in offshore waters. Acantharia and Foraminifera likely play important roles in NGA planktonic ecosystems because they were the most abundant group in their respective depth-niche and frequently participated in trophic interactions. Finally, this study provides images that can be used to communicate the existence of these unique organisms and as an identification tool for other Rhizaria researchers.

I. Comparison of NGA Rhizaria ecology to other oceanic systems

This study is one of seven reported to date that used Niskin bottle samples to obtain intact Rhizaria specimens (Michaels 1988, 1991, Gowing 1989, González 1992, Gowing and Garrison 1992, Michaels et al. 1995, Stoecker et al. 1996). This small number of studies affords few data for direct

comparison, especially since several (Michaels 1988, 1991, Stoecker et al. 1996) occurred in low latitude regions of the Atlantic and Pacific Oceans, systems that are distant and ecologically distinct from the NGA. There has not been a single analysis of Rhizaria ecology using Niskin bottles in the North Pacific north of the equator. Plankton net mesh sizes used in other studies were sometimes too large to capture smaller Rhizarians and juveniles, leaving out key portions of the population or even entire taxonomic groups that are sensitive to net tows in general, like Acantharia. Large Rhizarians, often rare or unevenly dispersed, are readily caught in plankton nets which might bias their perceived importance relative to the missed smaller cells. The Niskin bottle - 50 µm mesh - reverse filtration method utilized here resulted in unbiased collections from the water column and selected for the total Rhizaria size range, although the larger, rarer forms were not found given the relatively small volumes of water analyzed (~9 L per sample). Below we compare NGA Rhizaria communities to those from ocean systems alike (northwest North Pacific Ocean and Southern Ocean) and different from (equatorial Pacific, central North Pacific, and central North Atlantic) our study region. Numerous sediment trap studies have explored Rhizaria vertical flux, but they will not be discussed here. We consider studies that used net tow and Niskin sampling methods separately, given the different subsets of the Rhizaria community that they most effectively capture.

i. Plankton net tow method

Northwest North Pacific Ocean

The NGA Rhizaria community was similar to that of the northwest North Pacific (NP) region in terms of composition and vertical depth partitioning but differed by abundances and species diversity. There are just three reports on Rhizaria planktonic distribution in the northwest NP and, despite using the net tow method and analyzing much larger volumes of water, they are the most appropriate datasets to compare to the NGA because of proximity and ocean system similarity (Reshetnyak 1955, Okazaki et al. 2004, Ishitani and Takahashi 2007). The diversity and abundances of Radiolaria (likely Polycystina and Phaeodaria) in the Kuril-Kamchatka Deep were high in deeper waters (200-2000 m) (Reshetnyak 1955,

Casey 1971). In the Okhotsk Sea during late summer (Okazaki et al. 2004) and along the Japan coast during late spring (Ishitani and Takahashi 2007) Polycystine Radiolaria and Phaeodaria abundances were up to 3x lower (range <1.0-1.0 cell L^{-1}) than in the NGA (range <1.0-3.1 cells L^{-1}, Table 3). Abundance within these groups generally increased with depth to 100-200 m in the NP, whereas in the NGA, only a subset of Polycystines (Nassellaria) and Phaeodaria reliably followed this vertical trend. Species richness was substantially greater in the northwest NP, on the order of dozens of species. In contrast, we identified 31 Polycystina morphotypes and only four Phaeodaria (three Challengeridae and *P. acornis*) morphotypes (Figures 6 and 8, respectively). The Challengeridae family was an abundant Phaeodarian in all three northwest NP locations, as well as the NGA. Nassellaria were more abundant than Spumellaria on the Japan coastline (Ishitani and Takahashi 2007), which was also the case in the NGA (Table 3). These studies did not provide any data on Acantharia or Taxopodida Radiolarians for comparison. In general, the vertical depth niches of Polycystina and Phaeodaria were similar between the northwest NP and the NGA, while greater Rhizaria diversity was observed in the former region and greater abundances were observed in the latter region. The observation of higher species richness in the northwest NP is almost certainly a consequence of using plankton nets, which filter large volumes of water and can result in obtaining rarer or more dispersed individuals.

ii. Niskin bottle method

Southern Ocean

Rhizaria depth profiles in the NGA and Southern Ocean (SO) closely resembled each other, but there were several taxon-specific differences in community composition and abundance. Two studies that used a Niskin bottle sampling approach similar to ours, but with variable analyzed volumes, quantified Rhizaria distributions in the Weddell Sea during austral autumn (anywhere from 120 mL to 3.4 L) and winter (60 L). Total Rhizaria abundance during winter in the Weddell Sea (~ <1.0-8.0 cells L^{-1}, Gowing and Garrison 1992) was 3x lower than in the NGA (<1.0-25 cells L^{-1}, Figure 9a). "Small" Phaeodaria (<300 μm in autumn and <1.6 mm in winter) and *S. zanclea* were the most abundant Rhizaria in the SO, a

clear contrast with community structure in the NGA, where Acantharia was the dominant taxon. However, absolute abundances of small Phaeodaria were similar between the two high latitude oceans (<1.0-3.1 cells L^{-1}, Gowing 1989; <1.0-2.6 cells L^{-1}, Gowing and Garrison 1992; <1.0-3.1 cells L^{-1}, Challengeridae and *P. acornis*, Table 3). In the autumn study, these small Phaeodarians were sampled separately in net tows, but total volumes were small (5-7 L), while the winter study analyzed ~7x the volume we did (60 L) from bottles, which means we can confidently say NGA small Phaeodaria abundances were at the very least similar to, if not slightly greater than, the SO. Antarctic studies also identified low abundances (<1.0 cell L^{-1}) of large Phaeodaria (>300 µm in autumn and >1.6 mm in winter) from net samples. In autumn, total sample volume ranged from 166-400 L and in winter ~0.1 L. The small sample volumes we analyzed (~9 L) may explain why we did not encounter any large Rhizaria in the NGA. Recent studies using imaging technology (e.g. Underwater Vision Profiler, FlowCAM, Zooscan) such as Biard et al. (2016) reported global abundances of >600 µm Rhizaria as a percentage of the zooplankton community. The supergroup comprised on average 33% of the total zooplankton community in the upper 500 m. Remarkably, this study excluded a majority of the North Pacific from their analyses. Others have made quantifications using all three of the above instruments and reported that >200 µm Rhizarians were still <1.0 cell L^{-1} in the Mediterranean Sea (Llopis Monferrer et al. 2022).

There was a substantial difference in Acantharia abundances between the SO and NGA. In the Weddell Sea, Acantharians were up to 4 to 10x sparser during autumn and winter, respectively, than in the NGA (<1.0-2.8 cells L^{-1}, Gowing 1989; <1.0 cell L^{-1}, Gowing and Garrison 1992; <1.0-12 cells L^{-1}, Figure 9c). However, Gowing (1989) analyzed about 1/3 the volume we did, so Acantharia abundances may be similar in the SO autumn and NGA summer. Water column distributions were similar though; Acantharia generally increased with depth to around 100 m in both regions, although their depth maximum was shallower (30-40 m) in the SO during winter. Phaeodaria assemblages characteristically inhabited deep-water niches with numbers generally increasing with depth in both the SO and NGA. The Challengeridae family comprised a major portion of Phaeodarians in both high latitude regions, and small Phaeodarians contributed similar biomass to the Rhizarian community in the SO winter (max 0.0602 µg C

L^{-1}, Gowing and Garrison 1992) and NGA (max 0.0226 µg C L^{-1}, Challengeridae and *P. acornis*, GAK9 60-80 m, Table 4). Even at depths where Cercozoa made up fewer than 50% of the Rhizarian community by abundance in the NGA (Figure 10a), this phylum contributed substantially more biomass than abundant Acantharia Radiolarians because of their larger biovolumes. Most depths were influenced in this way by biomass of Challengeridae or *P. acornis* (Table 4). Distributions of Polycystina and *S. zanclea* were similar in the Weddell Sea and NGA, displaying increases with depth to about 150-250 m. *S. zanclea* abundances were at most 4x greater in the SO (max 4.2 cells L^{-1}, Gowing 1989; max 2.8 cells L^{-1}, Gowing and Garrison 1992; <1.0 cell L^{-1}, Table 3), while Polycystina numbers did not vary much across ecosystems. Foraminifera abundances were consistently low in the Weddell Sea (<1.0 cell L^{-1}, Gowing 1989, Gowing and Garrison 1992), despite the difference in sample volumes analyzed between the two seasons (up to ~ 3 L and 60 L, respectively), while in the NGA this group was up to 4x greater (<1.0-4.1 cells L^{-1}, Figure 9d). Unlike the decline with depth seen in the NGA (Figure 9d), Foraminifera did not exhibit a clear vertical gradient in Antarctic waters.

The Antarctic research discussed above demonstrates the similarities in Rhizaria assemblages between the NGA and SO in terms of species present and their water column distributions. Differences in abundances and dominant species were revealed, however. *S. zanclea* was more abundant in the SO and dominated the Rhizarian community along with Phaeodaria. Acantharia and Foraminifera were more abundant in the NGA, where the former group was the dominant taxon. Because these regions share subarctic/arctic characteristics like high productivity summers and iron-limited, high-nitrate low-chlorophyll (HNLC) offshore waters, SO Rhizaria assemblages might have reached similar abundances to those of the NGA if sampled during the spring or summer seasons of higher productivity.

Low latitude oceans

NGA Acantharia and Foraminifera abundances were like those of the equatorial Pacific (EP), but Foraminifera biomass was greater in the NGA. By concentrating 30 L Niskin water over mesh, Stoecker et al. (1996) found that in October at 0° 140°W, Acantharia abundances averaged about 8.0 cells L^{-1} and

Foraminifera 4.5 cells L^{-1} in the upper 90 m. In the NGA, abundances of Acantharia were at most 1.5x greater than in the EP, and Foraminifera were similar (surface to intermediate depths, <1.0-12 cells L^{-1}, Figure 9c and 1.0-4.1 cells L^{-1}, Figure 9d, respectively). However, we analyzed 3x less water than Stoecker et al. (1996) so it's possible that both groups were more abundant in the NGA. Both regions shared the same dominant taxa, the Acantharia. Again, taking into consideration sample volume, Acantharia biomass in these regions was similar (upper 100 m, 79 ng C L^{-1}, Table 4; upper 90 m, ~110 ng C L^{-1}, Stoecker et al. 1996), while NGA Foraminifera biomass was more clearly greater (350 ng C L^{-1}, Table 4; ~80 ng C L^{-1}, Stoecker et al. 1996). A similar size range of individuals were sampled in the NGA (>50 µm) and EP (>20 µm); most Foraminifera were >64 µm.

The depth-niche of Acantharia was deeper and more widespread in the NGA compared to another EP site, the Galapagos Vents (GV), but abundances were lower in our study region. Michaels (1988) also found that Acantharia were the dominant taxon. This study analyzed 2-5 L Niskin samples (1/5 to 1/2 of our analyzed volume) from the surface to 100 m at the GV in March. Acantharia abundances in the upper 20 m were up to 30x higher (range 1.70-28.6 cells L^{-1}) than in the NGA and declined with depth. Abundances were consistently low in the upper 20 m of the NGA (<1.0 cell L^{-1}, Figure 9c) but increased with depth. GV Acantharia peak abundance was 2x greater than in the NGA (28.6 cells L^{-1}, GV; 12 cells L^{-1}, NGA, Figure 9c). Despite major ecosystem contrasts, the Rhizarian community dominance of Acantharia was evident in the subpolar NGA and both EP sites.

NGA Rhizaria abundances were greater than, and vertical distributions were distinct from, those of the central NP and North Atlantic (NA) gyres. There was a stark contrast in the abundances and habitat of Acantharians. In the NGA summer, maximum Acantharia abundance was deeper and 3x higher compared to the NP gyre across multiple different seasons (~60-100 m, 12 cells L^{-1}, Figure 9c; <20 m, 4.1 cells L^{-1}, Michaels 1991). Michaels (1991) analyzed 10-12 L Niskin water. Lower abundances (max 5.5 cells L^{-1}) and a shallower depth niche for Acantharians was also seen in the NA central gyre (Sargasso Sea, 12 L Niskin samples analyzed) during spring and fall (Michaels et al. 1995). NA central gyre peak Foraminifera abundances were 4x lower than in the NGA (max 1.0 and 4.1 cells L^{-1}, respectively). This

group also didn't exhibit an obvious depth-niche like that seen in the NGA. Given these opposing vertical distributions and contrasting abundances, Acantharia and Foraminifera ecologies appear to differ between our mesotrophic subarctic study area and the lower latitude oligotrophic central gyres.

iii. Distribution patterns

NGA Rhizaria communities were influenced by depth. The communities residing at the surface differed from those occupying deeper waters, which was driven by Rhizaria phyla having distinct depth-niches. During the summer season, planktic Foraminifera dominated the surface, Radiolaria exhibited a more cosmopolitan vertical distribution, and Cercozoa usually resided below 60 m. It is not known exactly what controls the depth-niche partitioning of Rhizaria. Many researchers have attempted to compare Rhizaria vertical distributions to physical, chemical, or biological oceanographic parameters, to explain why these amoeboid protists live where they do. Associations have been made to temperature and salinity (Petrushevskaya 1971), carbon export (Guidi et al. 2016), potential prey (González 1992), salinity, chlorophyll-a, and dissolved oxygen (Ishitani and Takahashi 2007), and the Arctic Oscillation (Ikenoue et al. 2012). Others have suggested that distributions are influenced by seasonal hydrography (Casey 1971, Björklund 1974). To our knowledge, Rhizaria are unable to control their location in the water column in the way that non-gelatinous meso- and macrozooplankton do. Acantharia might be able to control buoyancy with contraction-relaxation cycles facilitated by non-actin myoneme organelles (Febvre 1981) and Taxopodida exhibit an oar-like rowing motion using non-actin contractile microfilament and microtubule axopods (Cachon et al. 1977). The relationship between distributions and environmental variables was not assessed here, mainly due to a lack of sample replication and the already distinct cross-shelf and water column gradients. Therefore, we hypothesize that Radiolaria and Cercozoa, which typically occur deeper than planktic Foraminifera, prefer to live well below the surface to avoid becoming stuck to particles and other plankton in the more particle-rich upper photic zone during the NGA's productive summer season. Foraminifera likely inhabit surface waters to maintain their associations with algal cells, whether those be mutualistic or commensal. Even though there was a deeper

pycnocline at GAK9 and GAK15 than at GAK1 and GAK5, most Radiolarians and Cercozoans persistently avoided depths above 30 m and 60 m, respectively, irrespective of station. Whether this indicates they were retained in the same water mass across the gulf, or simply are not found in shallower waters because they do not thrive there, is unknown. Rhizaria abundances and biomass generally increased with distance offshore in the NGA. This supports the current theory that Rhizaria prefer open ocean salinities (Boltovskoy et al. 2017) and could be why they were scarce at GAK1 (Figure 9a). Salinities were low in the upper 50 m at that station (Figure 2b; range 27.7-31.3) because of river and non-point source runoff transported by the Alaska Coastal Current (Figure 1).

The data we contributed from the subarctic region of the NGA contradicts the current understanding of Rhizaria biogeographical distributions. Rhizaria abundances and diversity are thought to be lowest at high latitudes and greatest in the equatorial regions (Casey 1966, 1971, Petrushevskaya 1971, Renz 1976, Be 1977). However, we provide evidence to the contrary. When generalizing the various results from two EP study areas, overall Rhizaria abundances in the NGA were similar to the equator. Moving northward to the central gyres, NGA abundances were markedly greater than the subtropical regions of the North Pacific and North Atlantic. Furthermore, Rhizaria abundances were greater in the NGA than other ecosystems at comparable high latitudes, including the Southern Ocean and northwest North Pacific Ocean. Data from studies like those compared here have supported the global biogeographical pattern stated above, of lower abundances nearer the poles. But the addition of this NGA dataset to the handful of high latitude reports calls into question the current paradigm. Thus, we propose a restructuring and refining of the Rhizaria equator-to-pole biogeographical gradient in the Pacific and Southern Oceans, as follows: abundances are high at the equator, decline in the subtropical gyres, and rise again with increasing proximity to the poles.

II. Trophic activities

i. Prey interactions

NGA Rhizaria prey capture incidence and range of prey types, which included diatoms, algal cells, other unidentified cells, ciliates, eggs, other Rhizarians, silicoflagellates, nauplii, and dinoflagellates, closely resembled those of two studies conducted in other oceans. Acantharians collected from the Gulf Stream and Sargasso Sea primarily preyed on diatoms and ciliates including tintinnids, while Foraminiferans in these areas were seemingly less selective and had a wider range of prey items including diatoms, eggs, gelatinous/soft zooplankton, fecal pellets, ciliates including tintinnids, and other Rhizarians (Swanberg and Caron 1991). That study reported roughly 40-50% of individuals with prey captured, whereas here we identified anywhere from 3.0-33%, depending on sample location (Figure 12a). SO Foraminifera, Taxopodida, and Phaeodaria held a variety of food items in digestive vacuoles such as diatoms, dinoflagellates, trichocysts and heterotrophic protists, <3 µm algae, Chlorella-like cells, bacteria, and other cellular or silicious fragments (Gowing 1986, 1989, Gowing and Garrison 1992). The same prey plus a few additional types were captured by NGA Rhizarians (Figure 12e). We hypothesize that prey items like phyto- and microzooplankton remain consistent even from opposite sides of the world because they share a size range with Rhizaria, and their prevalence allows for high likelihood of capture.

Vertical and cross-shelf trends were uncovered in the NGA whereby prey capture incidence generally declined with depth and, even more strongly, increased with distance offshore (Figure 12a). We hypothesize that prey capture was predominant at the surface because that is typically where phyto- and microzooplankton prey reside. Large cell (>20 µm) chlorophyll-a is representative of many phytoplankton species like diatoms, which was the most common prey type (Figure 12e). Maxima in >20 µm chlorophyll-a concentrations were between 10-30 m on the shelf and at 40 m off the shelf (Figure 2f). These depths largely coincide with the surface depth interval (0-20 m) that revealed the most individuals with prey captured (except offshore at GAK15). There is a higher probability of successful prey capture for a Rhizarian that lives in surface waters where large phytoplankton are most abundant. These amoeboid protists rely on algae for nutrition in the same way as heterotrophic or mixotrophic protists and

copepods, which are also prey items for Rhizaria. Since these plankton are more abundant near the surface, prey encounters are more likely to occur, even though Rhizaria abundances there were low (Figure 9a). Because Rhizaria abundances were highest in deeper waters but prey capture incidence was low there, we hypothesize that these organisms rely on obtaining nutrition from detritus and marine snow particles to survive below the photic zone. Prey capture incidence increased with distance from shore, a pattern that is surprising given the cross-shelf trend in Rhizaria abundances and our assumptions of prey availability. Prey capture was consistently high (range 25-33%, GAK15, Figure 12a) at depths above 100 m in the open ocean. Prey availability is presumably lower offshore compared to the shelf, due to the former being an iron-limited HNLC transition zone, but we do not have data to confirm this, so it remains unclear why Rhizaria predation was so successful at GAK15.

The taxonomic groups that consistently displayed the highest incidences of prey capture were Challengeridae, Foraminifera, and Acantharia (Figure 12c). Phaeodaria are thought to be non-selective feeders or even detritivores, as they are often found with unknown organisms captured or digesting amorphous material (Anderson 1983, Gowing 1986). González (1992) observed that Phaeodaria were important minipellet producers in the SO. We have evidence to support this idea because 6.3-24% of Challengeridae (including *P. acornis*) had captured unknown algal material that fluoresced red to yellow, indicative of photopigments, inside the phaeodium (Figure 12c). There are few data on the trophic biology and predator-prey interactions of the above groups, so further research is necessary to understand if different Rhizaria subgroups are selective feeders, generalists, and/or detritivores, and whether they compete for the same prey items.

We recognize the bias and possible errors in prey capture determinations in this work. At the very least, we presented quantitative and qualitative data to suggest the physical possibility of predator-prey interactions, even though the opportunities for predator-prey proximity and/or successful capture for the purposes of nutrient acquisition may have been encouraged through the multi-step concentration and settlement sample preparation process. This methodology could have allowed prey items to inadvertently stick to the cytoplasmic projections and spines of Rhizarians, facilitating interactions that were

independent of *in situ* prey capture at the time of sample collection. However, documentation of positive prey capture incidence was conservative, and all prey items identified here have been reported previously as stated above.

ii. Algal cell associations

The proportion of Rhizaria that interacted with algal cells generally decreased with depth and increased with distance offshore, remaining under 30% overall (Figure 12b). The highest incidences of algal associations occurred in shallow waters (above 50 m; Figure 12b). Rhizarians that maintain algae must reside where there is sufficient light for photosynthesis. The cross-shelf pattern is a bit more difficult to decipher. The offshore NGA waters are typically characterized as a transition region between the shelf and the iron-limited, HNLC waters of the subarctic gyre; one of only two high latitude HNLC regions along with the SO. In summer 2023, chlorophyll-a was low (Figure 2f,g) and nitrate was high (Figure 2d) at GAK15, indicative of an HNLC environment far offshore. Mixotrophic Rhizaria are important hubs of primary productivity with their symbionts in oligotrophic regions like the Sargasso Sea near Bermuda (Caron et al. 1995, Stoecker et al. 2017). We hypothesize that incidence of algal associations, whether those cells are endosymbionts or commensals, was higher seaward of the shelf break in the NGA because of the HNLC conditions present there. Mixotrophy could be a favorable trait for Rhizaria that live in the iron-limited offshore waters of the NGA because they can transition between nutrient acquisition modes depending on environmental conditions or prey availability. We hypothesize it may also be beneficial for microalgae to associate with large protists in these resource-limited regions if the host provides a livable microenvironment with waste products or other "leaking" carbon compounds that sustain the algal cells. Therefore, prevalence of mixotrophic Rhizaria may also be influenced by both organisms "seeking" benefits of the mutualistic partnership.

Foraminifera and Acantharia were the only taxonomic groups that consistently associated with algal cells (Figure 12d). However, Acantharia had fewer incidences of algal interactions than Foraminiferans. Numerous Acantharia, Polycystina, and Foraminifera species harbor algal symbionts,

whereas Phaeodaria are not known to partake in this trophic activity (Stoecker et al. 2009). It is not always clear whether associated algal cells are true endosymbionts, commensal or parasitic hitchhikers (Hemleben et al. 1989), prey, or even sequestered in an "inverted parasitism" relationship whereby only the host benefits, as suggested by Decelle (2013). Takagi et al. (2019) identified multiple Foraminifera species as having non-functional chlorophyll, which they hypothesized was derived either from prey items or aggregates at depth. Foraminifera algal associates include dinoflagellates as well as pelagophytes, chrysophytes, and *Synechococcus* spp. (Takagi et al. 2019). Acantharia symbionts are usually prymnesiophytes (Stoecker et al. 2009). Unfortunately, it was not possible to determine with our analyses, even broadly, what algal species were associated with NGA Rhizarians.

III. Conclusion

Our knowledge of Rhizaria is still at a beginning stage, but recent interest and technological advances have encouraged exciting new research to better understand the livelihoods of these unique amoeboid protists and their role in the global oceanic food web. This study provided a comprehensive view on Rhizaria ecology in the subarctic North Pacific with data that explained multiple facets of their ecology. Basic questions were answered: How many are there? What are their habitats? What do they look like? How big are they? What do they eat? We established baseline knowledge that can be expanded on in future NGA studies to explore how Rhizaria distributions, abundances, biomass, and diversity change seasonally and interannually. Our new subpolar dataset challenges the current consensus on biogeographical distribution in the Pacific and Southern Oceans. The existing idea is that abundances are highest near the equator and decrease toward the poles. Our data support a restructuring of this gradient, whereby abundances are high at the equator, low in the subtropical gyres, and rise again with increasing proximity to the poles, where abundances are similar to those of the equatorial region. This is an ambitious hypothesis due to the severe lack of research from different areas of the Pacific and Southern Oceans; for the data sets that do exist, contrasting methodologies and sampling seasons complicate direct comparisons. Many studies, including ours, lack replication and are temporally limited.

Thus, there is much work to be done across all oceans for scientists to fully comprehend the foundational aspects of Rhizaria biology and ecology.

Appendix

Supplemental Table 1. Biovolume measurement details.

Taxonomic group	Shape	Biovolume Equation	Dimensions
Unknown Rhizaria	spheroid	$4/3*\pi*r^3$	r=radius of central capsule
	prolate spheroid	$\pi/6*d^2*h$	d=shortest diameter of central capsule h=longest diameter of central capsule
Acantharia	spheroid	$4/3*\pi*r^3$	r=radius of central capsule
Polycystina	prolate spheroid	$\pi/6*d^2*h$	d=shortest diameter of skeleton h=longest diameter of skeleton
Spumellaria	spheroid	$4/3*\pi*r^3$	r=radius of medullary shell; if 2 shells, radius of inner medullary shell
Nassellaria			
umbrella-shaped	cylinder	$\pi*r^2*h$	r=longest radius of cephalis and/or thorax h=length from top of cephalis to bottom of abdomen
other shape or orientation	prolate spheroid	$\pi/6*d^2*h$	d=shortest diameter of skeleton h=length from top of cephalis to bottom of abdomen
	spheroid	$4/3*\pi*r^3$	r=radius of skeleton
Collodaria	spheroid	$4/3*\pi*r^3$	r=radius of central capsule
Sticholonche zanclea	prolate spheroid	$\pi/6*d^2*h$	d=shortest diameter of endoplasm h=longest diameter of endoplasm
Foraminifera	prolate spheroid	$\pi/6*d^2*h$	d=shortest diameter of chambers h=longest diameter of chambers
Challengeridae	prolate spheroid	$\pi/6*d^2*h$	d=shortest diameter of skeleton h=longest diameter of skeleton (not including oral spine)
Protocystis acornis	prolate spheroid	$\pi/6*d^2*h$	d=shortest diameter of skeleton h=longest diameter of skeleton (not including oral spine)

References

Anderson, O. R. 1983. Radiolaria. Springer New York, New York, NY.

Be, A. W. H. 1977. An ecological, zoogeographic and taxonomic review of recent planktonic Foraminifera. Pages 1–100 Oceanic Micropaleontology. Academie Press, London.

Becker, S., M. Aoyama, E. M. S. Woodward, K. Bakker, S. Coverly, C. Mahaffey, and T. Tanhua. 2020. GO-SHIP Repeat Hydrography Nutrient Manual: The Precise and Accurate Determination of Dissolved Inorganic Nutrients in Seawater, Using Continuous Flow Analysis Methods. Frontiers in Marine Science 7:581790.

Beers, J. R., F. M. H. Reid, and G. L. Stewart. 1975. Microplankton of the North Pacific central gyre. Population structure and abundance, June 1973. Internationale Revue der gesamten Hydrobiologie. 60:607–638.

Beers, J. R., F. M. H. Reid, and G. L. Stewart. 1977. Microplankton in the central gyre of the North Pacific Ocean. Part II: Population astructure and abundance. January-February 1973 (SOUTH TOW Expedition, leg 13), August-September 1973 (CLIMAX VII), March 1974 (TASADAY Expedition, leg 11), May 1974 (DRAMAMINE II). Institute of Marine Resources, University of California, San Diego, La Jolla, California.

Beers, J. R., F. M. H. Reid, and G. L. Stewart. 1982. Seasonal abundance of the microplankton population in the North Pacific central gyre. Deep Sea Research Part A. Oceanographic Research Papers 29:227–245.

Beers, J. R., and G. L. Stewart. 1970. The Preservation of Acantharians in fixed plankton samples. Limnology and Oceanography 15:825–827.

Beers, J. R., and G. L. Stewart. 1971. Micro-zooplankters in the plankton communities of the upper waters of the eastern tropical Pacific. Deep Sea Research and Oceanographic Abstracts 18:861–883.

Bernstein, R. E., P. R. Betzer, and K. Takahashi. 1990. Radiolarians from the western North Pacific Ocean: a latitudinal study of their distributions and fluxes. Deep Sea Research Part A. Oceanographic Research Papers 37:1677–1696.

Biard, T., J. W. Krause, M. R. Stukel, and M. D. Ohman. 2018. The Significance of Giant Phaeodarians (Rhizaria) to Biogenic Silica Export in the California Current Ecosystem. Global Biogeochemical Cycles 32:987–1004.

Biard, T., and M. D. Ohman. 2020. Vertical niche definition of test-bearing protists (Rhizaria) into the twilight zone revealed by in situ imaging. Limnology and Oceanography 65:2583–2602.

Biard, T., L. Stemmann, M. Picheral, N. Mayot, P. Vandromme, H. Hauss, G. Gorsky, L. Guidi, R. Kiko, and F. Not. 2016. In situ imaging reveals the biomass of giant protists in the global ocean. Nature 532:504–507.

BjÖrklund, K. R. 1974. The seasonal occurrence and depth zonation of radiolarians in Korsfjorden, Western Norway. Sarsia 56:13–42.

Boltovskoy, D., O. R. Anderson, and N. M. Correa. 2017. Radiolaria and Phaeodaria. Pages 731–763 Handbook of the Protists. 2nd edition. Springer International Publishing.

Boltovskoy, D., and N. Correa. 2016. Biogeography of Radiolaria Polycystina (Protista) in the World Ocean. Progress in Oceanography 149:82–105.

Boltovskoy, D., and N. Correa. 2017. Planktonic equatorial diversity troughs: fact or artifact? Latitudinal diversity gradients in Radiolaria. Ecology 98:112–124.

Boltovskoy, D., and S. S. Jankilevich. 1985. Radiolarian distribution in East equatorial Pacific plankton. Oceanologica Acta 8:101–123.

Boltovskoy, D., and W. R. Riedel. 1987. Polycystine radiolaria of the California Current region: Seasonal and geographic patterns. Marine Micropaleontology 12:65–104.

Bradshaw, J. S. 1959. Ecology of living planktonic Foraminifera in the North and equatorial Pacific Ocean. Contributions from the Cushman Foundation for Foraminiferal Research 10:25–69.

Cachon, J., and M. Cachon. 1978. Sticholonche zanclea Hertwig A Reinterpretation of its Phylogenetic Position Based Upon New Observations on its Ultrastructure. Archiv für Protistenkunde 120:148–168.

Cachon, J., M. Cachon, and L. G. Tilney. 1977. Movement Generated by Interactions between the Dense Material at the Ends of Microtubules and Non-Actin-Containing Microfilaments in Sticholonche zanclea. Journal of Cell Biology 72.

Caron, D. A., A. F. Michaels, N. R. Swanberg, and F. A. Howse. 1995. Primary productivity by symbiont-bearing planktonic sarcodines (Acantharia, Radiolaria, Foraminifera) in surface waters near Bermuda. Journal of Plankton Research 17:103–129.

Casey, R. E. 1966. A seasonal study on the distribution of Polycystine Radiolarians from waters overlying the Catalina Basin, Southern California. University of Southern California.

Casey, R. E. 1971. Distribution of polycystine Radiolaria in the oceans in relation to physical and chemical conditions. Pages 151–159 The Micropaleontology of Oceans. Cambridge University Press, London.

Cavalier-Smith, T. 1993. Kingdom Protozoa and Its 18 Phyla. MICROBIOL. REV. 57.

Cavalier-Smith, T. 2018. Kingdom Chromista and its eight phyla: a new synthesis emphasising periplastid protein targeting, cytoskeletal and periplastid evolution, and ancient divergences. Protoplasma 255:297–357.

Cavalier-Smith, T., E. E. Chao, and R. Lewis. 2018. Multigene phylogeny and cell evolution of chromist infrakingdom Rhizaria: contrasting cell organisation of sister phyla Cercozoa and Retaria. Protoplasma 255:1517–1574.

Cleveland, M. N. 1984. Radiolarian densities, diversities, and taxonomic composition in recent sediment and plankton of the southern California continental borderland: relationship to water circulation and depositional environments. Rice University, Houston, Texas.

Danielson, S. L., T. D. Hennon, D. H. Monson, R. M. Suryan, R. W. Campbell, S. J. Baird, K. Holderied, and T. J. Weingartner. 2022. Temperature variations in the northern Gulf of Alaska across

synoptic to century-long time scales. Deep Sea Research Part II: Topical Studies in Oceanography 203:105155.

Decelle, J. 2013. New perspectives on the functioning and evolution of photosymbiosis in plankton: Mutualism or parasitism? Communicative & Integrative Biology 6:e24560.

Decelle, J., S. Colin, and R. A. Foster. 2015. Photosymbiosis in Marine Planktonic Protists. Pages 465–500 *in* S. Ohtsuka, T. Suzaki, T. Horiguchi, N. Suzuki, and F. Not, editors. Marine Protists. Springer Japan, Tokyo.

Decelle, J., and F. Not. 2015. Acantharia. Pages 1–10 Encyclopedia of Life Sciences. First edition. Wiley.

Dorn, M., K. Aydin, B. Fissel, D. Jones, A. McCarthy, W. Palsson, and K. Spalinger. 2017. Assessment of the walleye pollock stock in the Gulf of Alaska. Stock Assessment.

Febvre, J. 1981. The myoneme of the Acantharia (Protozoa): A new model of cellular motility. Biosystems 14:327–336.

González, H. 1992. Distribution and abundance of minipellets around the Antarctic peninsula. Implications for protistan feeding behaviour. Marine Ecology Progress Series 90:223–236.

Gowing, M. M. 1986. Trophic biology of phaeodarian radiolarians and flux of living radiolarians in the upper 2000 m of the North Pacific central gyre. Deep Sea Research Part A. Oceanographic Research Papers 33:655–674.

Gowing, M. M. 1989. Abundance and feeding ecology of Antarctic phaeodarian radiolarians. Marine Biology 103:107–118.

Gowing, M. M., and D. L. Garrison. 1992. Abundance and feeding ecology of larger protozooplankton in the ice edge zone of the Weddell and Scotia Seas during the austral winter. Deep Sea Research Part A. Oceanographic Research Papers 39:893–919.

Gowing, M. M., and K. F. Wishner. 1986. Trophic relationships of deep-sea calanoid copepods from the benthic boundary layer of the Santa Catalina Basin, California. Deep Sea Research Part A. Oceanographic Research Papers 33:939–961.

Guidi, L., S. Chaffron, L. Bittner, D. Eveillard, A. Larhlimi, S. Roux, Y. Darzi, S. Audic, L. Berline, J. R. Brum, L. P. Coelho, J. C. I. Espinoza, S. Malviya, S. Sunagawa, C. Dimier, S. Kandels-Lewis, M. Picheral, J. Poulain, S. Searson, Tara Oceans Consortium Coordinators, L. Stemmann, F. Not, P. Hingamp, S. Speich, M. Follows, L. Karp-Boss, E. Boss, H. Ogata, S. Pesant, J. Weissenbach, P. Wincker, S. G. Acinas, P. Bork, C. de Vargas, D. Iudicone, M. B. Sullivan, J. Raes, E. Karsenti, C. Bowler, and G. Gorsky. 2016. Plankton networks driving carbon export in the oligotrophic ocean. Nature 532:465–470.

Gutierrez-Rodriguez, A., M. R. Stukel, A. Lopes dos Santos, T. Biard, R. Scharek, D. Vaulot, M. R. Landry, and F. Not. 2019. High contribution of Rhizaria (Radiolaria) to vertical export in the California Current Ecosystem revealed by DNA metabarcoding. The ISME Journal 13:964–976.

Haeckel, E. 1887. Report on the Radiolaria collected by H.M.S. Challenger during the years 1873-1876. 18:1–1803.

Hama, T., T. Miyazaki, Y. Ogawa, T. Iwakuma, M. Takahashi, A. Otsuki, and S. Ichimura. 1983. Measurement of photosynthetic production of a marine phytoplankton population using a stable 13C isotope. Marine Biology 73:31–36.

Hemleben, C., M. Spindler, and O. R. Anderson. 1989. Modern Planktonic Foraminifera. Springer-Verlag, New York.

Hillebrand, H., C.-D. Dürselen, D. Kirschtel, U. Pollingher, and T. Zohary. 1999. BIOVOLUME CALCULATION FOR PELAGIC AND BENTHIC MICROALGAE. Journal of Phycology 35:403–424.

Hopkins, T. L. 1985. Food web of an Antarctic midwater ecosystem. Marine Biology 89:197–212.

Hopkins, T. L. 1987. Midwater food web in McMurdo Sound, Ross Sea, Antarctica. Marine Biology 96:93–106.

Hopkins, T. L., and J. J. Torres. 1989. Midwater food web in the vicinity of a marginal ice zone in the western Weddell Sea. Deep Sea Research Part A. Oceanographic Research Papers 36:543–560.

Ikenoue, T., K. R. Bjørklund, A. K. Krabberød, S. Nishino, and P. Wassmann. 2023. Radiolaria and Phaeodaria (siliceous Rhizaria) in south-western and northern Norwegian fjords during late summer 2016: dominant species and biomass in shallow-water assemblages. Polar Research 42.

Ikenoue, T., K. Kimoto, Y. Okazaki, M. Sato, M. C. Honda, K. Takahashi, N. Harada, and T. Fujiki. 2019. Phaeodaria: An Important Carrier of Particulate Organic Carbon in the Mesopelagic Twilight Zone of the North Pacific Ocean. Global Biogeochemical Cycles 33:1146–1160.

Ikenoue, T., K. Takahashi, and S. Tanaka. 2012. Fifteen year time-series of radiolarian fluxes and environmental conditions in the Bering Sea and the central subarctic Pacific, 1990–2005. Deep Sea Research Part II: Topical Studies in Oceanography 61–64:17–49.

Imai, K., Y. Nojiri, N. Tsurushima, and T. Saino. 2002. Time series of seasonal variation of primary productivity at station KNOT (44°N, 155°E) in the sub-arctic western North Pacific. Deep Sea Research Part II: Topical Studies in Oceanography 49:5395–5408.

Ishitani, Y., and K. Takahashi. 2007. The vertical distribution of Radiolaria in the waters surrounding Japan. Marine Micropaleontology 65:113–136.

Itaki, T., K. Minoshima, and H. Kawahata. 2008. Radiolarian flux at an IMAGES site at the western margin of the subarctic Pacific and its seasonal relationship to the Oyashio Cold and Tsugaru Warm currents. Marine Geology 255:131–148.

Kimoto, K. 2015. Planktic Foraminifera. Pages 129–178 Marine Protists. Springer Japan.

Kling, S. A. 1966. Castanellid and Circoporid radiolarians: systematics and zoogeography in eastern north Pacific. University of California at San Diego.

Kling, S. A. 1979. Vertical distribution of polycystine radiolarians in the central North Pacific. Marine Micropaleontology 4:295–318.

Kling, S. A., and D. Boltovskoy. 1995. Radiolarian vertical distribution patterns across the Southern California current. Deep Sea Research Part I: Oceanographic Research Papers 42:191–231.

Kling, S. A., and D. Boltovskoy. 1999. Radiolaria Phaeodaria. Page 231 South Atlantic zooplankton. Backhuys Publishers, Leiden.

Krabberød, A. K., J. Bråte, J. K. Dolven, R. F. Ose, D. Klaveness, T. Kristensen, K. R. Bjørklund, and K. Shalchian-Tabrizi. 2011. Radiolaria Divided into Polycystina and Spasmaria in Combined 18S and 28S rDNA Phylogeny. PLoS ONE 6:e23526.

Krabberød, A. K., R. J. S. Orr, J. Bråte, T. Kristensen, K. R. Bjørklund, and K. Shalchian-Tabrizi. 2017. Single Cell Transcriptomics, Mega-Phylogeny, and the Genetic Basis of Morphological Innovations in Rhizaria. Molecular Biology and Evolution 34:1557–1573.

Laget, M., N. Llopis-Monferrer, J. Maguer, A. Leynaert, and T. Biard. 2023. Elemental content allometries and silicon uptake rates of planktonic Rhizaria: Insights into their ecology and role in biogeochemical cycles. Limnology and Oceanography 68:439–454.

Lampitt, R. S., I. Salter, and D. Johns. 2009. Radiolaria: Major exporters of organic carbon to the deep ocean: RADIOLARIA EXPORT CARBON TO THE DEEP OCEAN. Global Biogeochemical Cycles 23:n/a-n/a.

Lee, J. J., G. F. Leedale, and P. Bradbury, editors. 2000. The Illlustrated Guide to the Protozoa. Society of Protozoologists. Second edition. Allen Press Inc., Lawrence, KS.

Llopis Monferrer, N., T. Biard, M. M. Sandin, F. Lombard, M. Picheral, A. Elineau, L. Guidi, A. Leynaert, P. J. Tréguer, and F. Not. 2022. Siliceous Rhizaria abundances and diversity in the Mediterranean Sea assessed by combined imaging and metabarcoding approaches. Frontiers in Marine Science 9:895995.

Llopis Monferrer, N., S. Romac, M. Laget, Y. Nakamura, T. Biard, and M. M. Sandin. 2024. Gelatinous matrix, an original convergent evolution to cope with oligotrophy in Nassellaria (Radiolaria). preprint, Evolutionary Biology.

Mansour, J. S., A. Norlin, N. Llopis Monferrer, S. L'Helguen, and F. Not. 2021. Carbon and nitrogen content to biovolume relationships for marine protist of the Rhizaria lineage (Radiolaria and Phaeodaria). Limnology and Oceanography 66:1703–1717.

Michaels, A. F. 1988. Vertical distribution and abundance of Acantharia and their symbionts. Marine Biology 97:559–569.

Michaels, A. F. 1991. Acantharian abundance and symbiont productivity at the VERTEX seasonal station. Journal of Plankton Research 13:399–418.

Michaels, A. F., D. A. Caron, N. R. Swanberg, F. A. Howse, and C. M. Michaels. 1995. Planktonic sarcodines (Acantharia, Radiolaria, Foraminifera) in surface waters near Bermuda: abundance, biomass and vertical flux. Journal of Plankton Research 17:131–163.

Monferrer, N., D. Boltovskoy, P. Tréguer, M. M. Sandin, F. Not, and A. Leynaert. 2020. Estimating Biogenic Silica Production of Rhizaria in the Global Ocean. Global Biogeochemical Cycles 34.

Morley, J. J., and J. C. Stepien. 1985. Antarctic Radiolaria in Late Winter/Early Spring Weddell Sea Waters. Micropaleontology 31:365.

Munir, S., J. Rogers, X. Zhang, C. Ding, and J. Sun. 2020. The Horizontal Distribution of Siliceous Planktonic Radiolarian Community in the Eastern Indian Ocean. Water 12:3502.

Munir, S., J. Sun, and S. L. Morton. 2021. The First Record and Classification of Planktonic Radiolarian (Phylum Retaria) and Phaeodarian (Phylum Cercozoa) in the Eastern Indian Ocean. Biology 10:202.

Nakamura, Y., M. M. Sandin, N. Suzuki, A. Tuji, and F. Not. 2020. Phylogenetic Revision of the Order Entactinaria—Paleozoic Relict Radiolaria (Rhizaria, SAR). Protist 171:125712.

Nakamura, Y., and N. Suzuki. 2015. Phaeodaria: Diverse Marine Cercozoans of World-Wide Distribution. Pages 223–249 Marine Protists. Springer Japan.

Nigrini, C., and T. C. Moore, Jr. 1979. A Guide to Modern Radiolaria. Special Publication No. 16, Cushman Foundation for Foraminiferal Research.

Nikolaev, S. I., C. Berney, J. F. Fahrni, I. Bolivar, S. Polet, A. P. Mylnikov, V. V. Aleshin, N. B. Petrov, and J. Pawlowski. 2004. The twilight of Heliozoa and rise of Rhizaria, an emerging supergroup of amoeboid eukaryotes. Proceedings of the National Academy of Sciences 101:8066–8071.

Nishioka, J., H. Obata, T. Hirawake, Y. Kondo, Y. Yamashita, K. Misumi, and I. Yasuda. 2021. A review: iron and nutrient supply in the subarctic Pacific and its impact on phytoplankton production. Journal of Oceanography 77:561–587.

Okazaki, Y., K. Takahashi, T. Itaki, and Y. Kawasaki. 2004. Comparison of radiolarian vertical distributions in the Okhotsk Sea near the Kuril Islands and in the northwestern North Pacific off Hokkaido Island. Marine Micropaleontology 51:257–284.

Okazaki, Y., K. Takahashi, J. Onodera, and M. C. Honda. 2005. Temporal and spatial flux changes of radiolarians in the northwestern Pacific Ocean during 1997–2000. Deep Sea Research Part II: Topical Studies in Oceanography 52:2240–2274.

Okazaki, Y., K. Takahashi, H. Yoshitani, T. Nakatsuka, M. Ikehara, and M. Wakatsuchi. 2003. Radiolarians under the seasonally sea-ice covered conditions in the Okhotsk Sea: flux and their implications for paleoceanography. Marine Micropaleontology 49:195–230.

Oksanen J, Simpson G, Blanchet F, Kindt R, Legendre P, Minchin P, O'Hara R, Solymos P, Stevens M, Szoecs E, Wagner H, Barbour M, Bedward M, Bolker B, Borcard D, Carvalho G, Chirico M, De Caceres M, Durand S, Evangelista H, FitzJohn R, Friendly M, Furneaux B, Hannigan G, Hill M, Lahti L, McGlinn D, Ouellette M, Ribeiro Cunha E, Smith T, Stier A, Ter Braak C, Weedon J. 2024. vegan: Community Ecology Package. R package version 2.6-8, <https://CRAN.R-project.org/package=vegan>.

Petrushevskaya, M. G. 1971. Spumellarian and Nassellarian Radiolaria in the plankton and bottom sediments of the Central Pacific. Pages 309–317 The Micropaleontology of Oceans. Cambridge University Press, London.

Picheral, M., C. Catalano, D. Brousseau, H. Claustre, L. Coppola, E. Leymarie, J. Coindat, F. Dias, S. Fevre, L. Guidi, J. O. Irisson, L. Legendre, F. Lombard, L. Mortier, C. Penkerch, A. Rogge, C. Schmechtig, S. Thibault, T. Tixier, A. Waite, and L. Stemmann. 2022. The Underwater Vision Profiler 6: an imaging sensor of particle size spectra and plankton, for autonomous and cabled platforms. Limnology and Oceanography: Methods 20:115–129.

Picheral, M., L. Guidi, L. Stemmann, D. M. Karl, G. Iddaoud, and G. Gorsky. 2010. The Underwater Vision Profiler 5: An advanced instrument for high spatial resolution studies of particle size spectra and zooplankton. Limnology and Oceanography: Methods 8:462–473.

R Core Team. 2024. R: A Language and Environment for Statistical Computing. R Foundation for Statistical Computing, Vienna, Austria. <https://www.R-project.org/>.

Renz, G. W. 1976. The distribution and ecology of Radiolaria in the Central Pacific: plankton and surface sediments. University of California Press, Berkeley and Los Angeles, California.

Reshetnyak, V. V. 1955. Vertical distribution of radiolarians from the Kurilo-Kamchatka trench. Trudy Zoologicheskogo Instituta Academiya Nauk SSSR 21:94–101.

Schiebel, R., and C. Hemleben. 2005. Modern planktic foraminifera. Paläontologische Zeitschrift 79:135–148.

Stoecker, D., D. Gustafson, and P. Verity. 1996. Micro- and mesoprotozooplankton at 140*W in the equatorial Pacific: heterotrophs and mixotrophs. Aquatic Microbial Ecology 10:273–282.

Stoecker, D., M. Johnson, C. deVargas, and F. Not. 2009. Acquired phototrophy in aquatic protists. Aquatic Microbial Ecology 57:279–310.

Stoecker, D. K., P. J. Hansen, D. A. Caron, and A. Mitra. 2017. Mixotrophy in the Marine Plankton. Annual Review of Marine Science 9:311–335.

Stoecker, D., A. Taniguchi, and A. Michaels. 1989. Abundance of autotrophic, mixotrophic and heterotrophic planktonic ciliates in shelf and slope waters. Marine Ecology Progress Series 50:241–254.

Strom, S. 2023. Recent Marine Heatwaves Affect Marine Ecosystems from Plankton to Seabirds in the Northern Gulf of Alaska. Oceanography.

Strom, S., K. Bright, and K. Fredrickson. 2024. Widespread ciliate and dinoflagellate mixotrophy may contribute to ecosystem resilience in a subarctic sea: the northern Gulf of Alaska. Aquatic Microbial Ecology 90:1–21.

Strom, S. L., K. A. Fredrickson, and K. J. Bright. 2016. Spring phytoplankton in the eastern coastal Gulf of Alaska: Photosynthesis and production during high and low bloom years. Deep Sea Research Part II: Topical Studies in Oceanography 132:107–121.

Stukel, M. R., T. Biard, J. Krause, and M. D. Ohman. 2018. Large Phaeodaria in the twilight zone: Their role in the carbon cycle. Limnology and Oceanography 63:2579–2594.

Suzuki, N., and F. Not. 2015. Biology and Ecology of Radiolaria. Pages 179–222 Marine Protists. Springer Japan.

Suzuki, N., K. Ogane, Y. Aita, M. Kato, S. Sakai, T. Kurihara, A. Matsuoka, S. Ohtsuka, A. Go, K. Nakaguchi, S. Yamaguchi, T. Takahashi, and A. Tuji. 2009. Distribution Patterns of the Radiolarian Nuclei and Symbionts Using DAPI-Fluorescence.

Swanberg, N. R. 1983. The trophic role of colonial Radiolaria in oligotrophic oceanic environments. Limnology and Oceanography 28:655–666.

Swanberg, N. R., and D. A. Caron. 1991. Patterns of sarcodine feeding in epipelagic oceanic plankton. Journal of Plankton Research 13:287–312.

Takagi, H., K. Kimoto, T. Fujiki, H. Saito, C. Schmidt, M. Kucera, and K. Moriya. 2019. Characterizing photosymbiosis in modern planktonic foraminifera. Biogeosciences 16:3377–3396.

Takahashi, K. 1987. Radiolarian flux and seasonality: Climatic and El Nino response in the subarctic Pacific, 1982-1984. Global Biogeochemical Cycles 1:213–231.

Takahashi, K. 1997. Time-series fluxes of Radiolaria in the eastern subarctic Pacific Ocean. News of Osaka Micropaleontologists 10:299–309.

Takahashi, K., and S. Honjo. 1981. Vertical Flux of Radiolaria: A Taxon-Quantitative Sediment Trap Study from the Western Tropical Atlantic. Micropaleontology 27:140.

Takahashi, K., and H. Y. Ling. 1980. Distribution of Sticholonche (Radiolaria) in the upper 800 m of the waters in the Equatorial Pacific. Marine Micropaleontology 5:311–319.

Takahashi, O., S. Mayama, and A. Matsuoka. 2003. Host-symbiont associations of polycystine Radiolaria: epifluorescence microscopic observation of living Radiolaria. Marine Micropaleontology 49:187–194.

Takami, M., and A. Fukui. 2012. Ontogenetic development of a rare liparid, Paraliparis dipterus, collected from Suruga Bay, Japan, with notes on its reproduction. Ichthyological Research 59:134–142.

Welling, L. A., N. G. Pisias, and A. K. Roelofs. 1992. Radiolarian microfauna in the northern California Current System: indicators of multiple processes controlling productivity. Geological Society, London, Special Publications 64:177–195.